Predicting Exchange Coupling in Molecular Systems with Density Functional Theory

Master's Thesis
University of Jyväskylä
Department of Chemistry
6th July 2021
Juho M. Toivola

Abstract

Density Functional Theory has become a well-established approach among modern quantum chemistry theories due to its relatively low computational cost compared to many wave function-based methods. After the introduction of molecular magnetism and exchange-coupled molecular systems, density functional theory has proven to be suitable for accurately determining the strength and type of exchange coupling based on molecular energies. In validation studies it has been shown that the right combination of exchange-correlation functional and basis set can provide exchange coupling constants that are in good agreement with experimental data, although the performance of different combinations can vary tremendously. In this work, the theory of density functional theory and magnetism are reviewed, focusing on exchange coupling and how modern density functional approaches can succeed in delivering accurate exchange coupling constants.

Tiivistelmä

Tiheysfunktionaaliteoria on ottanut paikkansa vakiintuneena kvanttikemian työkaluna sen laskennallisen tehokkuutensa ansiosta verrattuna moniin aaltofunktiomenetelmiin. Molekyylimagnetismin ja vaihtokytkettyjen molekylaaristen systeemien keksimisen jälkeen tiheysfunktionaaliteoria on osoittautunut erinomaiseksi menetelmäksi vaihtokytkennän suuruuden ja tyypin määrittämiseen molekyylien energioiden pohjalta. Validointikokeet ovat osoittaneet, että oikea vaihtokorrelaatiofunktionaalin ja kantajoukon yhdistelmä voi tuottaa vaihtokytkentävakioita, jotka ovat lähellä kirjallisuusarvoja, vaikka eri yhdistelmien suorituskyky voikin vaihdella suuresti. Tässä työssä tarkastellaan tiheysfunktionaaliteorian ja magnetismin teoriaa keskittyen vaihtokytkentään, ja siihen, miten nykyiset tiheysfunktionaalimenetelmät onnistuvat tuottamaan tarkkoja kytkentävakioita.

Preface

Most of the writing for this thesis was done between May 1st and June 12th, 2021, under the guidance of Academy of Finland Research Fellows Dr. Jani O. Moilanen and Dr. Akseli Mansikkamäki. This thesis considers the background, theory, and current methods used in density functional theory, and the role of exchange coupling in magnetism, especially molecular magnetism, and how it can be probed using density functional methods. In terms of source material, basic information was gathered from textbooks and review articles. This basic understanding was supplemented by primary literature mainly searched with Google Scholar, Scopus, and www-browsers.

I would like to express my gratitude to my supervisors, Jani O. Moilanen and Akseli Mansikkamäki, for their enthusiasm and superb guidance on the topic, the personnel of the Main Group Chemistry research group at JYU for creating an encouraging and supportive atmosphere in which it has been a pleasure to work, and my friends and family for supporting me throughout my studies and choices. Assistant Professor Dr. Antti Karttunen is also warmly acknowledged for evaluating this work. I also want to thank the Department of Chemistry at JYU and the Academy of Finland (project 320015) for funding the computational project related to my thesis that allowed me to branch out into computational chemistry and work remotely during the pandemic.

July 6, 2021, Jyväskylä

Juho M. Toivola

TABLE OF CONTENTS

List of Abbreviations and Acronyms

AFM	antiferromagnetic
BS	broken symmetry
CAM	Coulomb attenuation method
CASSCF	complete active space self-consistent field
CGF	contracted Gaussian function
CSF	configuration state function
DFT	density functional theory
DHF	Dirac–Hartree–Fock
DKH	Douglas–Kroll–Hess
DZ	double-ζ
ECP	effective core potential
EPR	electron paramagnetic resonance
FM	ferromagnetic
GEA	gradient expansion approximation
GGA	generalized-gradient approximation
GTO	Gaussian-type orbital
HDvV	Heisenberg–Dirac–van Vleck
HF	Hartree–Fock
HH	half-and-half
HK	Hohenberg–Kohn
HS	high-spin
IS	intermediate-spin
KS	Kohn–Sham
LCAO	linear combination of atomic orbitals
LDA	local density approximation
LSDA	local spin-density approximation
MO	molecular orbital
QTM	quantum tunnelling of magnetization
QZ	quadruple-ζ
RHF	restricted Hartree–Fock
RKS	restricted Kohn–Sham
ROHF	restricted open-shell Hartree–Fock
RSH	range-separated hybrid

SCF	self-consistent field
SIM	single-ion magnet
SMM	single-molecule magnet
SOMO	singly-occupied molecular orbital
SQUID	superconducting quantum interference device
STO	Slater-type orbital
SV	split valence
TF	Thomas–Fermi
TZ	triple-ζ
UHF	unrestricted Hartree–Fock
UKS	unrestricted Kohn–Sham
VB	valence bond
XC	exchange-correlation
ZORA	zeroth-order regular approximation

1 Introduction

Density functional theory[1–4] (DFT) has attracted substantial attention since the mid-1960s, and it experienced a surge in popularity among quantum chemists in the 1990s. With current density functional methods, it is possible to investigate large systems that would be inconvenient to compute with most wave function-based methods. This computational affordability has been one of the key characteristics responsible for the success of DFT.

Computational chemistry approaches are based on the concept of solving the Schrödinger equation approximately for many-electron systems such as atoms and molecules. In one of the simplest wave-function based approaches—the Hartree–Fock (HF) method—the many-electron wave function is treated as a Slater determinant.[5,6] The Slater determinant is a mathematical representation of noninteractive fermionic—in quantum chemistry, electronic—wave functions, which allows its Schrödinger equation to be solved iteratively. The major drawback of the HF scheme is a considerable discrepancy between the predicted energy and the true energy of the system, called correlation energy, which arises from the simplification of the wave function. Unlike wave function-based approaches, DFT methods focus on instead calculating the energy of a system by varying its electron density, which drastically reduces the number of variables needed. Modern DFT is rooted in two theorems proposed by Hohenberg and Kohn[1] in 1964. These theorems validated the use of electron density as the sole variable for calculating the energies corresponding to the electron densities, analogous to solving the Schrödinger equation. Earlier density functional approaches such as the Thomas–Fermi model[7,8] were insufficient for anything but crude, qualitative results, notably due to their inaccurate representation of kinetic energy. Then came Kohn and Sham[2] who proposed a computationally accessible and, in principle, exact method for using functionals to calculate the energy of a given density. In the Kohn–Sham (KS) scheme, only the bare minimum of the energy functional is approximated, and a portion of kinetic energy that is approximated, for example, in the Thomas–Fermi (TF) model is calculated from a Slater determinant that corresponds to the electron density of the system under investigation. The approach proposed by Kohn and Sham was a revolutionary piece of theory that opened a pathway for the development of sophisticated, approximate exchange-correlation functionals that are used in DFT today.

The KS scheme introduces a reference system of noninteractive electrons, a Slater determinant, to DFT, from which a large portion of the kinetic energy is calculated exactly. The exchange-correlation functionals in the KS approach describe all the contributions to the energy functional that are unknown and need to be approximated. This consists of the exchange and correlation energies that are not contained in the density or the non-interacting reference system.

Electron exchange refers to effects that arise from the antisymmetry in relation to the exchange of two electrons. Electron correlation includes all energy contributions that arise from the individual motion of the electrons, such as dispersion. In exchange-correlation (XC) functionals these effects are often represented by using the so-called XC hole. This hole is a function that describes a region of space that contains a deficiency of one electron, relative to a reference electron from which the hole originates. The only instance in which the exchange-correlation hole is well-known is in a density that represents a uniform electron gas, in other words a constant density. This concept was used in the first exchange-correlation functional, called a local density approximation (LDA),[2] in which every point in the electron density is treated locally as being part of a uniform electron gas. This representation is simple and clean, but it suffers from the inability to accurately describe systems, such as molecules, in which the electron density varies rapidly. LDA was followed by generalized-gradient approximations (GGAs), in which not only the density is treated locally, but also its gradient, which allows rapidly varying densities to be accurately described. As a tradeoff, the exchange-correlation holes that emerge from this approximation are unphysical and need to be manually adjusted. Nevertheless, GGAs are often used as the building blocks of modern exchange-correlation functionals such as hybrid functionals that treat a portion of the electron exchange exactly by incorporating the Hartree–Fock exchange term.

As with any quantum chemistry method, the system investigated with DFT needs to be parameterized in a way that can be computed. This is done by writing the wave function as a finite set of basis functions that represent the one-electron wave functions in the system.[3] These basis functions can have analytical form or be completely numerical. There are various types of basis sets, each with their pros and cons. The Gaussian-type orbitals (GTOs) are well-defined, and important integrals between these GTOs can be calculated exactly. However, the GTOs are poor representations of physical electron wave functions as they lack important characteristics such as derivative discontinuity at the center of an atom. The drawbacks of GTOs can be counteracted by representing each wave function as a linear combination of GTOs, which also increases the computational cost. Slater-type orbitals (STOs) are the opposite in the sense that they are good representations of physical wave functions, but their integration must be done numerically. Numerical basis sets, however, are flexible and can be arbitrarily accurate, but they also involve hard-to-calculate integrals and, thus, are computationally expensive. Additionally, the numerical bases must contain a large amount of volume elements to produce accurate data. These basis sets allow the problem of finding the ground state electron density to be solved almost entirely by matric equations and linear algebra, which is well-suited for modern computational infrastructures.

DFT has also been used to probe the magnetic properties of molecules and materials.[9,10] Magnetism is a phenomenon that has been known for centuries but the origins of which remained elusive until the 20th century. It is now well known that magnetism is caused by the magnetic moments arising from angular momentum and spin quantum numbers of particles, often limited to unpaired electrons in chemistry.[11] These magnetic moments linked to the states of the electrons can exhibit long-range ordering, which is the main mechanism behind magnetic properties such as ferromagnetism. Long-range ordering of magnetic moments between electrons is caused by the exchange coupling between the spins of these electrons. Theoretically, exchange coupling has two components: The exchange integral term contributing to ferromagnetic (FM) exchange coupling, and the overlap integral term which promotes antiferromagnetic (AFM) coupling. In FM coupling, two magnetic moments are aligned parallel, while in AFM coupling, they align antiparallel. The strength and type (AFM or FM) of these couplings are determined by so-called exchange coupling constants.[12]

In DFT and other quantum chemistry methods, exchange coupling constants can be calculated by various means. In most of these approaches, the energies of a system are calculated in different spin states, and the exchange coupling constants are derived from the differences in energy. The Heisenberg–Dirac–van Vleck[13] (HDvV) Hamiltonian provides a way of calculating the exchange coupling constants based solely on the energies of the different magnetic states, by projecting each magnetic moment along one axis. These methods involving the HDvV Hamiltonian often rely on broken symmetry[3,14–18] (BS) approaches that account for not only the energies, but also the spin of each magnetic state, eliminating some of the problems posed by the presence of higher spin multiplicities—known as spin contamination—in unrestricted Hartree–Fock (UHF) and unrestricted Kohn–Sham (UKS) schemes. Still, the excited magnetic states cannot fully be described by individual Slater determinants, which is often seen as a limiting factor for the accuracy of these methods for probing exchange coupling.

There are various types of systems that involve exchange coupling. These systems almost exclusively fall under the field of molecular magnetism. Molecular magnetism is a field that focuses on magnetism that originates from molecular structures. One of the earliest groups of hypothetical molecules that started the field consisted of organic ferromagnets.[19] The field then expanded to also cover transition metal assemblies, and single-molecule magnets. Exchange coupling has been an important quality in determining the utility of organic radical-based materials and transition metal clusters, and more recently it has been incorporated into some lanthanide-based single-molecule magnets, too. Computational chemistry calculations, including DFT, have provided considerable information regarding the exchange coupling in

these systems, and it could potentially be used in predicting these features in hypothetical molecules.

The aim of this work is to provide a clear picture of DFT, and how it can be used to predict exchange coupling in molecular systems. Chapter 2 focuses on the background and theory of DFT. Additionally, it introduces the reader to current methods used in DFT. Chapter 3 elucidates the mechanisms behind magnetism and exchange coupling, and methods for calculating exchange coupling constants based on computational data. Chapter 4 reviews the field of molecular magnetism, and it describes creative uses of DFT to calculate exchange coupling constants in molecular magnets. Throughout this work, most quantities are represented in atomic units, where physical constants such as Dirac's constant, elementary charge, electron mass, and Coulomb constant are set to unity and thus do not appear in the equations.

2 Density Functional Theory

In the field of chemistry, DFT comprises a variety of methods with the goal of circumventing the task of solving a Schrödinger equation for the electrons in a molecule. DFT methods accomplish this by substituting the wave function approach of solving the Schrödinger equation with an alternative method of instead optimizing the electron density that describes the same system. This chapter aims to review the origins, theory, and current methods of DFT from a chemistry point of view.

2.1 Origins of DFT

The principal problem that DFT seeks to solve is as old as quantum mechanics itself. Ever since the introduction of the Schrödinger equation in the early 1920s, researchers have investigated alternative methods for finding solutions to it for complex systems. In quantum chemistry, a large amount of interest in the Schrödinger equation lies in its time-independent form

$$\hat{\mathrm{H}}\Psi = E\Psi, \tag{1}$$

where $\hat{\mathrm{H}}$ is the Hamiltonian, and E is the energy of the wave function Ψ. With currently available methods, equation (1) can only be solved analytically for simple systems, such as a free electron, an electron in an infinite potential well, a hydrogen atom, or a H_2^+-ion by using the Born-Oppenheimer approximation, where the nuclei are treated as static compared to the electrons due to the large difference between their masses.[11] The reason why the Schrödinger equation cannot be solved analytically for complex systems lies in the definitions of the wave function and the Hamiltonian; when two particles interact, their wave functions and the energy depend on each other's variables, too. In the nomenclature of differential equations, this

situation corresponds to whether it is possible to solve the differential equation by separation of variables. In further discussion, the Born–Oppenheimer approximation is generally assumed, as it is widely involved in the basic idea of DFT and virtually all quantum chemistry methods.[3]

The Born–Oppenheimer approximation is a famous tool in chemistry for investigating electronic structures. In it, the positions of nuclei are fixed, and electrons are allowed to move freely.[3,11,20] The justification for this approximation lies in the largely different masses between nuclei and electrons, with the former being upwards of 1800 times more massive, depending on the atomic number. Therefore, the greater inertia of the nuclei causes them to move considerably slower than the electrons. The power of this approximation results from the large reduction in complexity with the smaller drawback of not accounting for motion-induced interactions between electrons and nuclei.

The limitations of solving the Schrödinger equation prompted the search for alternative, approximate methods for finding solutions. One of the earliest methods adopted in quantum chemistry is the variational principle. In quantum mechanics, the variational principle states that the true ground state wave function of the system is the one which minimizes the energy of the Schrödinger equation.[3,11] Therefore, one can systematically construct wave functions that approach the minimum energy given by the Schrödinger equation, and thus converge on the true ground state wave function of the system. This is because the true ground state wave function is always lower in energy than any trial wave function. On its own, the variational principle has little practical value, but over time it has shown to be a powerful tool in virtually all quantum chemistry methods, because it allows the use of approximate wave functions and constrains the energies given by these wave functions in the Schrödinger equation.

2.1.1 Hartree–Fock Approach

One idea to simplify the task of solving the Schrödinger equation in the early years of quantum mechanics was to approximate the total electronic wave function as a product of many individual wave functions

$$\Psi(\vec{x}_1, \vec{x}_2, \dots, \vec{x}_N) = \psi_1(\vec{x}_1) \cdot \psi_2(\vec{x}_2) \cdot \dots \cdot \psi_N(\vec{x}_N), \qquad (2)$$

where Ψ is the approximate total electronic wave function, and ψ_i are the single single-electron wave functions with coordinates $\vec{x}_i$, which contain both the spatial coordinates and the spin coordinate. Equation (2) is generally known as the Hartree approximation.[21] It was shown that the Hartree approximation in conjunction with the variational principle could be used to describe systems more complex than atoms.[5,6] This approach involved replacing the single-electron wave functions in equation (2) with a determinant of such functions. The determinant meets the criteria of the Pauli principle without adding much complexity, when the product of

the total wave functions is antisymmetric with respect to the exchange of two wave functions. These determinants are now known as Slater determinants

$$\Phi_{\mathrm{SD}} = \frac{1}{\sqrt{N!}} \begin{vmatrix} \chi_1(\vec{x}_1) & \chi_2(\vec{x}_1) & \cdots & \chi_N(\vec{x}_1) \\ \chi_1(\vec{x}_2) & \chi_2(\vec{x}_2) & \cdots & \chi_N(\vec{x}_2) \\ \vdots & \vdots & \ddots & \vdots \\ \chi_1(\vec{x}_N) & \chi_2(\vec{x}_N) & \cdots & \chi_N(\vec{x}_N) \end{vmatrix}, \quad (3)$$

where $\chi_i(\vec{x}_j)$ are spin orbitals in which $\vec{x}_j$ are composed of both the spatial and spin coordinates of the electron, and N is the total number of one-fermion wave functions in the system. This definition of the wave function is widely used among quantum chemistry methods today. In essence, the slater determinant is another description for the total electronic wave function of a noninteractive system and allows a systematic way for generating approximate wave-functions to be used in the variational principle. In the HF method, the spin orbitals in the Slater determinant are varied under the constraint that they conserve orthonormality.[i] A Hamiltonian is then used to find the energies of these variations, and the variation with the lowest energy represents the best HF approximation for the ground state wave function of the system. Additionally, because the HF energy of the wave function depends on the spin orbitals, and in the Slater determinant orthonormality is conserved, it is possible to determine the energies of the individual spin orbitals using equations called Hartree–Fock equations

$$\hat{\mathrm{f}}\,\chi_i = \varepsilon_i \chi_i, \quad (4)$$

where $\hat{\mathrm{f}}$ is the Fock operator which is a one-electron energy operator, and ε_i are eigenvalues that represent orbital energies.[3,22] Generally, the HF equations (Eq. 4) are used to first find the minimum energies for the orbitals, which are in turn used to construct the Slater determinant (Eq. 3). One particularly significant quality of the HF method from the perspective of DFT is the elimination of self-interaction. As will be shown later in this chapter, the integration of exchange effects to DFT is a considerable challenge due to the self-interactions involved with electron density. The basic principles of the HF method have many similarities to DFT in that the wave function, in this case the Slater determinant (Eq. 3) describes a set of noninteractive fermions that instead interact with potentials generated by them, much like the densities of individual electrons in DFT interact with the total electron density they represent. As such, many features of the HF method were adopted in the development of DFT, which is explained in more detail in chapter 2.2. In many quantum chemistry software used today, KS-DFT and HF calculations are very similar, and HF can be considered as a special case of KS-DFT, where the density portion of the calculation is nonexistent.

[i] This condition ensures that the wave functions remain physically meaningful.

Electron correlation is a term that was first introduced in the context of the HF method as correlation energy, the error of the HF energy based on the variational principle.[3,23] This quantity describes all the energy contributions that are not accounted for in the HF method, including the true movement of the electrons affecting Coulomb interactions (dynamic correlation) and dissociation of bonds at large distances (static correlation). In addition to these types of correlation energy, there are contributions to the energy arising from the kinetic and potential terms that result from the approximation of the wave function. Correlation energy that appears in the Kohn–Sham method has many similarities to the HF electron correlation energy and will be discussed further in chapter 2.2.

A concept that was introduced with the HF method that also has applications in other quantum chemistry methods, including DFT, is the concept of restricted and unrestricted HF models.[3,24] A large proportion of molecules in nature are covalent, closed shell systems, meaning that all the spatial orbitals in the molecule are doubly occupied. Therefore, it is sensible to restrict the spatial orbitals in the system to either be empty or doubly occupied. This approximation in the context of the HF method is called the restricted Hartree–Fock (RHF) model. It is apparent that RHF is not suitable for molecules with an odd number of electrons, or in general molecules with non-singlet ground states. There are two ways to handle the singly occupied orbitals: One method, called the restricted open-shell Hartree–Fock model[25] (ROHF) restricts the occupancy of all other orbitals, while the more commonly used UHF model allows the spin orbitals to have a different shape, size and potential. The main difference between ROHF and UHF is that in UHF, the α- and β-spin densities are defined separately by forming Fock operators for each spin, while in ROHF the Fock operators are formed separately for closed shell and open shell electrons. Therefore, UHF is simpler but also has the disadvantage that the unrestricted orbitals can cause the Slater determinant to be contaminated so that it corresponds more with higher spin-multiplicity wave functions, and thus the determinant is not an eigenfunction of the total spin operator. in ROHF, this problem is mostly eliminated, as only the open shell is treated as such, but this introduces theoretical problems regarding the invariance—in other words, the property to remain unchanged—of orbitals under certain matrix transformations commonly used in quantum chemistry software.

A couple of years before the HF method was developed, a self-consistent field (SCF) was first mentioned, and it is commonly used in the HF method to solve the HF equations to find the orbital energies.[21] The idea behind this self-consistent field method was to start with an estimation of a field including all nuclei and electrons in a system and calculate the single-electron wave functions of the electrons in this field. This process is repeated until the input field and the output field are the same for the electronic wave function, within numerical

boundaries. As will become apparent in the later parts of this thesis, self-consistent field methods have also become an essential part of modern DFT methods.

2.1.2 Electron Density and Hole Functions

Another idea for finding approximate solutions to the Schrödinger equation involved substituting the wave function of electrons with electron density. Despite their limited usefulness, the first density functional methods, including the famous TF model, were proposed in the late 1920s.[7,8] The benefit of using density as a variable over wave functions is the reduction in the number of spatial variables from $3N$ to just 3; electron density can be expressed as a function with three spatial variables based on a wave function according to

$$\rho(\vec{r}) = N \int \dots \int |\Psi(\vec{x}_1, \vec{x}_2, \dots, \vec{x}_N)|^2 ds_1 d\vec{x}_2 \dots d\vec{x}_N. \quad (5)$$

where ρ is electron density, N is the number of electrons, and $\Psi(\vec{x}_1, \vec{x}_2, \dots, \vec{x}_N)$ is the total electronic wave function. In equation (5), the integration over all spin variables and all but one set of spatial variables means that only one set of spatial variables, $\vec{r}$, remains. This derivation results in a model that is significantly simpler and can be measured experimentally, for instance with x-ray diffraction experiments. However, replacing the wave function with density brought its own challenges. With introducing density as an alternative variable came the tasks of designing approximate functionals capable of eliminating self-interactions between the densities of individual electrons and the total density, and incorporating the quantum interactions into the model, notably exchange interactions and Coulomb correlation.[4] Exchange interaction is a statistic, purely quantum mechanical effect that relates to the Pauli principle and describes the change in total energy that nearby, identical fermions, such as electrons, experience.[26] Exchange interaction is discussed further in chapter 3. Definitions of electron correlation in literature vary between authors, so in this work, three definitions are used regarding different concepts containing the word correlation. First, electron correlation is used to refer to the Coulombic correlation between electrons. Second, exchange-correlation is used as a term that combines Coulombic and Fermi correlation terms. Third, correlation energy is reserved to describe the difference between the true energy of a ground state and an energy given by the HF or KS methods.

The first steps towards bridging the gaps between the wave function and electron density approaches emerged soon after the concepts were first conceived.[7,8] In 1933, the concept of a Fermi, or exchange hole, was introduced. Mathematically, this hole is a function that gives the probability of finding an electron of parallel spin as a function of distance from a fixed reference electron.[3,4,27] In terms of electron density, the hole can be thought of as a region of space that

contains a deficiency of an elementary charge in the region described by the hole function. For DFT, the Fermi, or exchange hole[28] was an important step in the integration of electronic exchange to the method, and it inspired new interpretations for exchange interactions in quantum chemistry approaches that later also affected DFT.[4,28,29] Furthermore, the concept of an exchange hole was generalized into the XC hole with the addition of the coulomb hole.[2–4,30] The XC hole contains both the exchange-hole and the coulomb hole, and it describes a region in the electron density where there is deficiency of one elementary charge due to a combination of the Pauli exclusion principle and the coulomb repulsion. Between the exchange and Coulomb holes, the exchange hole dominates at short distances (low delocalization), whereas the role of the Coulomb hole is to mitigate the Coulombic self-interaction and correct the electron dissociation discussed earlier in the context of the HF method. Unlike the exchange hole which integrates to -1, the Coulomb hole integrates to zero over all space. The hole functions have been very important for DFT in the effort to eliminate the non-physical self-interactions, and to integrate exchange interaction and electron correlation into the model.

Mathematically, the XC hole functions used in modern DFT have six spatial and two spin coordinates.[3] This is because in order for such a hole function to contain electron-electron interaction terms, it must originate from the spin pair density, a mathematical construct in which the electron density is defined as

$$\rho_2(\vec{x}_1, \vec{x}_2) = N(N-1) \int \dots \int |\Psi(\vec{x}_1, \vec{x}_2, \dots, \vec{x}_N)|^2 d\vec{x}_3 \dots d\vec{x}_N. \quad (6)$$

This is similar to the electron density in equation (5), with the exception that it contains all the information needed to account for electron-electron interactions, namely exchange and correlation. While the electron density (Eq. 5) represents a probability of finding an electron with arbitrary spin at position $\vec{r}$, the spin pair density tells us the probability of simultaneously finding an electron at position $\vec{r}_1$ with spin s_1 and another electron at position $\vec{r}_2$ with spin s_2. The effects of exchange and correlation can be separated from equation 6 by writing the spin pair density as

$$\rho_2(\vec{x}_1, \vec{x}_2) = \rho(\vec{x}_1)\, \rho(\vec{x}_2) \left(1 + f(\vec{x}_1, \vec{x}_2)\right), \quad (7)$$

where $f(\vec{x}_1, \vec{x}_2)$ is called the correlation factor, and it includes the interactions between electrons 1 and 2. In a completely noninteractive system, in other words when the correlation factor is zero, the spin pair density in equation (7) integrates to N^2 over the electron coordinates. This is problematic because the true description of the spin pair density (Eq. 6) integrates to $N(N-1)$, which indicates that the separated equation should contain self-interactions.[ii] This

[ii] Self-interaction occurs between the density generated by an individual electron and the total density.

brings us to the concept of the XC hole function and its mathematical definition in the spin pair density

$$h_{\mathrm{XC}}(\vec{x}_1,\vec{x}_2) = \frac{\rho_2(\vec{x}_1,\vec{x}_2)}{\rho(\vec{x}_1)} - \rho(\vec{x}_2) = \Omega(\vec{x}_1,\vec{x}_2) - \rho(\vec{x}_2)$$
$$= \rho(\vec{x}_2)\, f(\vec{x}_1,\vec{x}_2), \qquad (\mathbf{8})$$

where the fraction, or conditional probability Ω, represents the probability of finding an electron with coordinates $\vec{x}_2$ when there is another electron with coordinates $\vec{x}_1$. As mentioned before, the exchange-correlation hole contains a deficiency of one electron, in other words it integrates to -1, which can also be derived from equation (8); the conditional probability integrates to $N-1$ because $\vec{x}_2 \neq \vec{x}_1$, and the density term to just N. This description of the exchange-correlation hole also shows that the hole can have any shape, depending on the electron density, or more specifically, the spin pair density. From looking at equation (8), it becomes apparent how the spin pair density and hole functions can be utilized in solving the self-interaction problem and including electron-electron interactions into an electron density model, but it is not yet clear how it directly fits into DFT without further discussion, which is provided in Chapter 2.3.

2.1.3 Hohenberg–Kohn Theorems

Advancements with electron density culminated in two breakthroughs that led to massive improvements in practical DFT methods. The first one was the DFT formalism proposed by Hohenberg and Kohn in 1964[1], and the second one was the approach created by Kohn and Sham (see chapter 2.2).[2] The main goal of the Hohenberg–Kohn (HK) theorems was to prove the viability of density as a variable by showing that the density uniquely determines all the properties of the system.[1,3,4] They solved the problems of relating the total electronic wave function to electron density in two steps: In the first theorem, they showed that the external potential $V_{\mathrm{ext}}(\vec{r})$ (disregarding the constant term) in the Hamiltonian $\hat{\mathrm{H}}$ is a unique functional of the ground state electron density $\rho(\vec{r})$. Because $V_{\mathrm{ext}}(\vec{r})$ fixes $\hat{\mathrm{H}}$, the energy of the total ground state electronic wave function Ψ must also be a unique functional of $\rho(\vec{r})$. Therefore, the non-degenerate ground state electronic wave function is uniquely determined by the ground state electron density, which in turn determines all the properties of the system. In the second theorem, they proved that there is a universal functional that is independent of the external potential which satisfies a variational principle linking the minimum of the energy functional to the ground state electron density. In other words, they proved that there is a mathematical expression that establishes a unique correspondence between the energy of a system and

electron density, and that this expression gives the ground state energy and electron density at its minimum. This expression is the universal functional

$$F_{HK}[\rho] = \langle \Psi | \hat{T} + \hat{E}_{ee} | \Psi \rangle = T[\rho] + E_{ee}[\rho], \quad (9)$$

where $\hat{T}$ is the kinetic energy operator and $\hat{E}_{ee}$ is the operator for all electron-electron interaction energies, and $T[\rho]$ and $E_{ee}[\rho]$ are their respective functionals. This functional in theory could solve the exact energy of a system so that the Schrödinger equation could also be solved exactly. Obviously, the exact form of this functional is not known beyond being non-analytical and non-local, even though it has been shown to exist. Instead, there are alternative approaches for approximating the functional. The HK theorems were generalized to apply to all densities that can be derived from Slater determinants by Levy and Lieb.[31,32] It should be mentioned that the HK theorems or those proposed by Levy and Lieb do not guarantee that the derivative of the energy functional exists, which is important for practical calculations.

A caveat of approximating the true universal functional is that the variational principle no longer applies. One can obtain energies lower than the true ground state energy, and the energy obtained using the functional does not necessarily converge towards the ground state density.[1] In many ways, DFT is an approximate, practical quantum chemistry method that focuses more on being versatile and efficient rather than being accurate, but more and more sophisticated functionals are being developed constantly. It should be emphasized that the HK theorems are merely mathematical proofs, and by themselves cannot be used for practical calculations. However, these theorems are considered by many to be the foundation for today's DFT methods, in addition to Levy's and Lieb's theories, because practically all DFT methods that have been developed since rely on what these two theorems prove. To be clear, density functional methods like the Thomas–Fermi model already existed, but the HK theorems validated DFT and future work to be done in the field.[3,4]

In addition to the theoretical formulation of DFT, there was plenty of work to implement DFT methods feasible for practical computation. The other major contribution towards establishing DFT as the practical method it is today was done by Kohn and Sham,[2] who introduced a more practical description of the energy functional and developed what are now known as the Kohn–Sham equations—equations that are similar to the HF equations but use electron density as the basic variable instead of wave functions.

2.2 The Kohn–Sham Approach

One year after the publishing of the HK theorems, the second breakthrough in DFT was achieved by Kohn and Sham.[2] They realized that most problems with density functional methods in those days involved the way the kinetic energy was defined.[3,7,8,33] This led to a large

approximation in the kinetic energy term, which rendered available methods virtually useless in anything but rough, qualitative analyses. Kohn and Sham also realized that this approximation is not present in wave function-based approaches, such as the HF method.[5,6] These observations inspired them to create a method, in which a wave function-based reference system is used to calculate as much of the kinetic energy exactly as possible, so that the portion of the kinetic energy that needs to be approximated is minimized. This approach proved to be so effective that DFT methods used today almost exclusively rely on the Kohn–Sham scheme.

The HK theorems published a year prior showed that electron density could be used as the basic variable to solve many-body systems. The solutions offered could in theory be exact, as evidenced by the existence of a universal functional F[ρ]. This universal functional contains all the energy contributions of the true system

$$\mathrm{F}[\rho(\vec{r})] = \mathrm{T}[\rho(\vec{r})] + \mathrm{U}[\rho(\vec{r})] \qquad (\mathbf{10})$$

where $\mathrm{T}[\rho]$ is the true kinetic energy functional, $\mathrm{U}[\rho]$ is the potential energy functional. In most density functional methods at the time, both the kinetic energy functional $\mathrm{T}[\rho]$ and the potential energy functional $\mathrm{U}[\rho]$ were approximated entirely as explicit functionals of electron density, which resulted in the limited accuracy of these methods. The ingenuity in the KS approach was to alter the universal functional where only the necessary part of the kinetic energy functional $\mathrm{T}[\rho]$ would have to be approximated, based on the knowledge that wave function models, notably the HF method, were able to handle kinetic energy exactly. This brings us to the reference system introduced in the KS approach.

To calculate some of the kinetic energy exactly, Kohn and Sham devised a reference system that bears a close resemblance to the approximation of the total electronic wave function in the HF method. Recall from chapter 2.1.1 that the total electronic wave function can be expressed as a collection of many single-electron wave functions, as described by the Hartree approximation. These single electron wave functions can be combined to a Slater determinant (Eq. 3) which represents a system of noninteractive electrons that is antisymmetric relative exchange of two electrons, or rows or columns in the matrix. In principle, the Slater determinant is an exact wave function of a system, where the electrons do not interact with each other through Coulomb repulsion. The most important quality of Slater determinants for the KS approach is the ability to express the kinetic energy of such a system,

$$\mathrm{T_{HF}} = -\frac{1}{2}\sum_{i}^{N}\langle\chi_i|\nabla^2|\chi_i\rangle, \qquad (\mathbf{11})$$

exactly. Kohn and Sham utilized this approach to construct a reference system of non-interactive electrons that instead interact with an effective potential that is both local and multiplicative, and it generates the same electron density as the true system. Importantly, this

reference system can be represented as a Slater determinant, which would allow them to calculate most of the kinetic energy exactly.[2,3] To do this, a Hamiltonian

$$\hat{\mathrm{H}}_{\mathrm{S}} = -\frac{1}{2}\sum_{i}^{N}\nabla_i^2 + \sum_{i}^{N}\mathrm{V}_{\mathrm{S}}(\vec{r}_i), \tag{12}$$

was constructed for the reference system. This Hamiltonian contains a kinetic energy term and a potential term that do not include interactions between electrons. Therefore, the ground state wave function can be represented as a Slater determinant (Eq. 3), where the spin-orbitals can be determined from

$$\hat{\mathrm{f}}_{\mathrm{KS}}\phi_i = \varepsilon_i\phi_i, \tag{13}$$

where $\hat{\mathrm{f}}_{\mathrm{KS}}$ is the one electron Kohn–Sham operator

$$\hat{\mathrm{f}}_{\mathrm{KS}} = -\frac{1}{2}\nabla^2 + \mathrm{V}_{\mathrm{S}}(\vec{r}), \tag{14}$$

analogous to equation (4). To ensure that this reference system works for calculating the kinetic energy contribution excluding interactions, a condition is imposed, where the electron density arising from the reference system ρ_{S} must correspond to the ground state electron density ρ_0 of the true system according to

$$\rho_{\mathrm{S}}(\vec{r}) = \sum_{i}^{N}\sum_{s}|\phi_i(\vec{r},s)|^2 = \rho_0(\vec{r}). \tag{15}$$

With the reference system established, Kohn and Sham showed that it is possible to separate the universal functional into a set of known and unknown functionals

$$\mathrm{F}[\rho(\vec{r})] = \mathrm{T}_{\mathrm{S}}[\rho(\vec{r})] + \mathrm{J}[\rho(\vec{r})] + \mathrm{E}_{\mathrm{XC}}[\rho(\vec{r})], \tag{16}$$

where $\mathrm{E}_{\mathrm{XC}}[\rho]$ is defined as exchange-correlation energy functional, containing all the potential and kinetic energy contributions that arise from exchange, correlation, and self-interaction correction, similar to how HF correlation energy is defined as all the contributions that are not included in the model.[2,3] $\mathrm{T}_{\mathrm{S}}[\rho]$ is the exact kinetic energy of the reference system borrowed from the HF analogue in equation (11)

$$\mathrm{T}_{\mathrm{S}} = -\frac{1}{2}\sum_{i}^{N}\langle\phi_i|\nabla^2|\phi_i\rangle. \tag{17}$$

Even though the density does not appear explicitly in the reference system, it can be rationalized that its kinetic energy T_{S} must be an implicit functional of energy density. By looking at equation (9), one can see that the total energy of the reference system depends only on the kinetic energy of the system and the external potential, which is a functional of the electron density. According to the HK theorems, the total ground state energy must be a unique functional of electron density. Therefore, if the kinetic energy was not a functional of electron

density, there would not be a unique mapping of ground state energy and electron density demanded by the HK theorems. One important element in the KS approach remains: how to define the external potential so that it provides a density identical to our true system (Eq. 15)?

The external potential can be derived by first expanding the total energy functional of the system based on equation (16)

$$\begin{aligned} &\mathrm{E}[\rho(\vec{r})] = \mathrm{T_S}[\rho(\vec{r})] + \mathrm{J}[\rho(\vec{r})] + \mathrm{E_{XC}}[\rho(\vec{r})] + \mathrm{E_{Ne}}[\rho(\vec{r})] \\ &= -\frac{1}{2}\sum_{i}^{N}\langle\phi_i|\nabla^2|\phi_i\rangle + \frac{1}{2}\sum_{i}^{N}\sum_{j}^{N}\iint|\phi_i(\vec{r}_1)|^2\frac{1}{r_{12}}\left|\phi_j(\vec{r}_2)\right|^2 d\vec{r}_1\, d\vec{r}_2 \\ &+\mathrm{E_{XC}}[\rho(\vec{r})] - \sum_{i}^{N}\int\sum_{A}^{M}\frac{Z_A}{r_{1A}}|\phi_i(\vec{r}_1)|^2\, d\vec{r}_1, \end{aligned} \tag{18}$$

where the electron-nucleus attraction term $\mathrm{E_{Ne}}[\rho]$ has been added. By applying the variational principle to find the orbitals that yield the minimum energy,[3,34] equation (18) transforms to a set of coupled one-electron equations

$$\begin{aligned} &\left(-\frac{1}{2}\nabla^2 + \left[\int\frac{\rho(\vec{r}_2)}{r_{12}}d\vec{r}_2 + \mathrm{V_{XC}}(\vec{r}_1) - \sum_{A}^{M}\frac{Z_A}{r_{1A}}\right]\right)\phi_i = \varepsilon_i\phi_i \\ &\left(-\frac{1}{2}\nabla^2 + \mathrm{V_{eff}}\right)\phi_i = \varepsilon_i\phi_i, \end{aligned} \tag{19}$$

where one gets the form for the Kohn–Sham operator (Eq. 13) and finds a formula for the external potential (Eq. 14). Equations with the form in equation (19) are generally called Kohn–Sham equations, and they provide a means for calculating the external potential and ultimately, a solution to the Schrödinger equation. In theory, the method is exact, but because the exchange-correlation terms are unknown, they must be approximated, and because the external potential is a functional of the electron density, and the electron density is affected by the potential, it must be solved in a self-consistent fashion. Modern density functional methods are based on the design of approximate exchange-correlation functionals, and the design of new, more accurate approximate exchange-correlation functionals is a central part of theoretical DFT research.

It should be noted that as well as the HF method, Kohn–Sham approach only uses a single determinant, where all the information can be drawn from. In this sense, it is susceptible to some of the same pitfalls as RHF and UHF.[3] Much like in RHF and UHF, the conditions used for the calculation in KS-DFT can involve restricted or unrestricted spin orbitals (RKS or UKS respectively). Like RHF, RKS is limited in correctly mimicking dissociation and non-singlet spin multiplicities. Likewise, UKS may involve the spin contamination of the system due to higher multiplicities available when unrestricted orbitals are used. Contrary to HF, these

limitations are not innate to the KS theory; as evidenced by the HK theorems, the KS theory is exact under the condition that the true XC functional is used, and thus KS is, in theory, able to provide the same energies given by the Schrödinger equation. Instead, these shortcomings appear with the introduction of approximate XC functionals. Therefore, for practical applications, open-shell systems call for so-called spin-density functionals that define the external potential separately for both spin densities.

RKS formalism is relatively straightforward. The effective potential of the KS equations is solved without considering the spin of the electrons. Instead, the KS orbitals appear as doubly degenerate pairs, each of which can contain up to two electrons.[3] Even in systems where there is an odd number of electrons, the total density is the only important variable, and the individual spin densities are disregarded. In principle, this is enough to obtain the energy of any arbitrary spin multiplicity, but as one could gather from the previous paragraph, approximate spin-density functionals are needed for practical open-shell calculations.

2.3 Approximate Exchange-Correlation Functionals

With wave function-based computational methods, the accuracy of the calculation solely depends on the wave function used. Therefore, the key to increasing the accuracy of wave function-based methods is to create trial wave functions that correspond better and better to nature in terms of their observable characteristics. Indeed, there is a systematic way for generating more accurate wave functions. Recall from chapter 2.1.1 that in the HF scheme, the wave function is a linear combination of single-electron wave functions, a Slater determinant. The HF approach represents the basic level of wave function-based methods, in a wider hierarchy of so-called configuration interaction methods.[3] Another way to define the wave function is as a linear combination of Slater determinants that is an eigenfunction of the spin operator—a configuration state function (CSF). This is one way to approximate the complete configuration interaction, where the wave function is an infinite cascade of linear combinations. In practical calculations, a finite number of orbitals is used, with the size of the computation increasing rapidly with the size of the basis set, in other words the amount of basis functions to describe the orbitals. Generating the wave function as a linear combination of all possible basis functions in a finite basis set is called full configuration interaction, and it is a common wave function-based method that is applicable to small systems. Therefore, by following this procedure of generating trial wave functions, one can arrive at arbitrary accuracy at the cost of exponentially increasing complexity.

The configuration interaction hierarchy for wave-function based methods enables the systematic construction of more and more accurate wave functions, because the accuracy of the

calculation depends only on the wave function used. In contrast, the accuracy of density functional methods depends only on the functional used, and there is no systematic way of creating more accurate functionals.[3] However, this opens an opportunity for innovation in the design of better exchange-correlation functionals for KS-DFT. The lack of a systematic approach to improving the accuracy of XC functionals has led many functionals being viable, each with their advantages and disadvantages. The following discussion focuses on advancements in the design of approximate XC functionals.

First, some clarification on the hole functions is needed for the context of XC functionals. The XC hole is a function of the spin pair density that describes a region of space where there is a deficiency of exactly one electron. It contains the potential energy contributions from electron-electron interactions by being a function of the space and spin coordinates of two electrons. However, as was shown in the KS approach, the exchange and correlation contributions are not exclusive to the potential energy; there is also the kinetic exchange-correlation term. So, is there a way to integrate the kinetic correlation into the XC hole? The answer to this question comes in the form of the adiabatic connection.[3,35] Consider the two systems in the KS scheme: the non-interacting reference system, and the fully interacting true system. These systems can be expanded into a continuum of partially interacting systems by introducing a coupling strength parameter and writing the Hamiltonian of the system as

$$\hat{\mathrm{H}}_{\lambda} = \hat{\mathrm{T}} + \lambda\hat{\mathrm{V}}_{\mathrm{ee}} + \hat{\mathrm{V}}_{\mathrm{ext}}^{\lambda}, \tag{20}$$

where λ is the coupling strength parameter ranging from 0 to 1, $\hat{\mathrm{T}}$ and $\hat{\mathrm{V}}_{\mathrm{ee}}$ are the kinetic and potential energy operators, and $\hat{\mathrm{V}}_{\mathrm{ext}}^{\lambda}$ is an external potential that is adjusted to retain the density of the fully interacting system with each λ. With $\lambda = 0$ and $\lambda = 1$ this equation becomes

$$\begin{aligned} \hat{\mathrm{H}}_{\lambda=0} &= \hat{\mathrm{T}} + \hat{\mathrm{V}}_{\mathrm{ext}}^{\lambda=0} = \hat{\mathrm{T}} + \hat{\mathrm{V}}_{S} \\ \hat{\mathrm{H}}_{\lambda=1} &= \hat{\mathrm{T}} + \hat{\mathrm{V}}_{\mathrm{ee}} + \hat{\mathrm{V}}_{\mathrm{ext}}^{\lambda=1} = \hat{\mathrm{T}} + \hat{\mathrm{V}}_{\mathrm{ee}} + \hat{\mathrm{V}}_{\mathrm{eff}}, \end{aligned} \tag{21}$$

where $\hat{\mathrm{H}}_{\lambda=0}$ and $\hat{\mathrm{H}}_{\lambda=1}$ are the Hamiltonians for the non-interacting reference system and the fully interacting true system, respectively. From looking at equation (21), it is not yet obvious how kinetic correlation is included. Now we use the adiabatic connection to write the energy of the interacting system as

$$\mathrm{E}_{\lambda=1} = \mathrm{E}_{\lambda=0} + \int_{0}^{1} d\mathrm{E}_{\lambda}. \tag{22}$$

The next step is to define $d\mathrm{E}_{\lambda}$. The corresponding Hamiltonian can be written as

$$d\hat{\mathrm{H}}_{\lambda} = d\hat{\mathrm{V}}_{\mathrm{ext}}^{\lambda} + \hat{\mathrm{V}}_{\mathrm{ee}} d\lambda. \tag{23}$$

This representation can be expanded to give the differential energy $d\mathrm{E}_{\lambda}$, in which the exchange-correlation term can be expressed in the hole formalism

$$dE_\lambda = \int \rho(\vec{r}) d\hat{V}_{ext}^{\lambda} d\vec{r} + \frac{1}{2} d\lambda \iint \frac{\rho(\vec{r}_1)\rho(\vec{r}_2)}{r_{12}} d\vec{r}_1 d\vec{r}_2 + \frac{1}{2} d\lambda \iint \frac{\rho(\vec{r}_1) h_{XC}^{\lambda}(\vec{x}_1, \vec{x}_2)}{r_{12}} d\vec{x}_1 d\vec{x}_2, \quad (24)$$

where $h_{XC}^{\lambda}(\vec{x}_1, \vec{x}_2)$ is the coupling strength-dependent exchange-correlation hole. By substituting this into equation (22) and expanding the $E_{\lambda=0}$ term the equation transforms into

$$E_{\lambda=1} = T_S + \int \rho(\vec{r}) V_{eff} d\vec{r} + \frac{1}{2} \iint \frac{\rho(\vec{r}_1)\rho(\vec{r}_2)}{r_{12}} d\vec{r}_1 d\vec{r}_2 + \frac{1}{2} \iint \frac{\rho(\vec{r}_1) \bar{h}_{XC}(\vec{r}_1, \vec{r}_2)}{r_{12}} d\vec{r}_1 d\vec{r}_2, \quad (25)$$

where T_S is the kinetic energy of the non-interacting reference system and $\bar{h}_{XC}$ is the coupling strength-integrated exchange-correlation hole

$$\bar{h}_{XC}(\vec{r}_1, \vec{r}_2) = \int_0^1 h_{XC}^{\lambda} \, d\lambda. \quad (26)$$

Equation (25) shows how the energy of the fully interacting system can be written as the sum of the kinetic energy of the reference system, the coulombic interaction term including the unphysical self-interaction, and the coupling strength-integrated XC hole.[3] Therefore, the hole function must also contain the kinetic energy contribution from exchange and correlation. Even though this approach complicates the XC hole, it should now be obvious how the exchange-correlation hole is significant for KS-DFT, as modern functionals can utilize the hole function to describe all the problematic terms in the energy functional. Here, we explored the idea of applying the adiabatic connection to the non-interacting reference system and to the actual, fully interacting system in KS-DFT to integrate the kinetic correlation term into the XC hole. The focus now shifts to the development of functionals, but the concept of the coupling strength-integrated exchange-correlation hole will be important in the discussion to follow.

The first approximate exchange-correlation functional to be proposed for KS-DFT was done by Kohn and Sham themselves in their landmark paper.[2] They proposed an energy functional for the homogeneous electron gas, in which the electrons are placed on a positive background, so that the combined system is electrically neutral.[2,3] The background consists of constant electron and proton densities and hole functions for each electron. While this type of model is very different from the quickly varying electron densities seen in molecules, it is the only density for which nearly exact XC functionals are known. Therefore, it has become the basis from which nearly all approximations are derived from. The simplest such derivation is the local density approximation (LDA). Mathematically, LDA can be represented as

$$\mathrm{E}_{\mathrm{XC}}^{\mathrm{LDA}}[\rho(\vec{r})] = \int \rho(\vec{r})\varepsilon_{\mathrm{XC}}[\rho(\vec{r})]\, d\vec{r}$$
$$\mathrm{E}_{\mathrm{XC}}^{\mathrm{LSDA}}[\rho_\alpha, \rho_\beta] = \int \rho(\vec{r})\varepsilon_{\mathrm{XC}}[\rho_\alpha(\vec{r})\rho_\beta(\vec{r})]\, d\vec{r}, \quad (\mathbf{27})$$

where $\varepsilon_{\mathrm{XC}}[\rho(\vec{r})]$ is the exchange-correlation potential experienced by an electron in a field of constant density at the point $\vec{r}$ in the actual density $\rho(\vec{r})$; in other words, the local electron density around each point in space is extended over all space to form a constant density, and the energy is calculated in the potential that arises from this constant density. $\mathrm{E}_{\mathrm{XC}}^{\mathrm{LSDA}}[\rho_\alpha, \rho_\beta]$ represents the local spin-density approximation[3] (LSDA), in which the electron density is separated to spin densities ρ_α and ρ_β to account for spin polarization.

In both LDA and LSDA, hole functions are employed within the $\varepsilon_{\mathrm{XC}}$ terms to eliminate the self-interaction and account for exchange and correlation. Because the density is set to be constant around every point, the hole functions are spherically symmetric and have relatively simple forms. One might wonder how either of these drastic approximations can be of any use for molecular systems. Surprisingly, LDA can provide quite accurate data on the structure and vibrations of molecules.[3] Some qualitative reasons behind its successes include that the hole functions chosen meet important criteria including

$$\lim_{r_2 \to r_1} h_{\mathrm{X}}(r_1, r_2) = -\rho(r_1), \quad (\mathbf{28})$$

indicating that the combined system of constant density and the exchange hole is consistent with the Pauli exclusion principle. Additionally, the spherical symmetry, in other words, the isotropy of the LDA exchange-correlation hole does not necessarily affect the results. This is because the LDA hole can lead to the same energy as an anisotropic one, when its value at any arbitrary radius is the corresponding radial average of the anisotropic hole. However, the position of the LDA hole tends to be more disconnected from nuclei relative to the more realistic, anisotropic hole, which often leads to LDA overestimating bond energies because the electrons are more localized to the bonds in LDA. In Summary, the LDA hole functions are relatively simple, which eases calculations, but at the same time they lose accuracy over longer distances, which renders them insufficient for predicting specific chemistry related data such as bond energies. LDA can still provide consistent data on some molecular properties such as structure, vibrations, and more specific data when the system under investigation is relatively close to the LDA model, for example solid metals and simple crystalline solids.

2.3.1 Generalized Gradient Approximations

Beyond local density approximations, the next step towards suitable approximations for molecular systems comes in the form of generalized gradient approximations (GGAs).[3,36] As

expected, these approximations consider not only the value of the density at each point, but also the gradient. As such, they can better represent systems that involve faster-varying electron densities, such as molecules. To see how GGAs can be derived from local spin-density approximations, let us start by looking at gradient expansion approximations (GEAs)

$$\begin{aligned} \mathrm{E}_{\mathrm{XC}}^{\mathrm{GEA}}[\rho_\alpha, \rho_\beta] &= \int \rho(\vec{r}) \varepsilon_{\mathrm{XC}}[\rho_\alpha(\vec{r}) \rho_\beta(\vec{r})] d\vec{r} \\ &+ \sum_{\sigma,\sigma'} \int \mathrm{C}_{\mathrm{XC}}^{\sigma,\sigma'}[\rho_\alpha(\vec{r}), \rho_\beta(\vec{r})] \frac{\nabla\rho_\sigma(\vec{r})}{\rho_\sigma(\vec{r})^{\frac{2}{3}}} \frac{\nabla\rho_{\sigma'}(\vec{r})}{\rho_{\sigma'}(\vec{r})^{\frac{2}{3}}} d\vec{r}, \end{aligned} \tag{29}$$

where $\nabla\rho(\vec{r})$ is the gradient of the electron density, and σ and σ' denote spin α or β. This approximation is obviously more complex than the simple local density approximations, but it often underperforms in comparison. This can be explained with the properties of the hole functions in both approximations. In LDA, the exchange and correlation holes integrate to -1 and 0, respectively, and the exchange hole is negative everywhere. Neither of these conditions is necessarily met by the hole functions in GEA.

The shortcomings of the gradient expansion approximations due to poorly defined hole functions can be solved by altering the holes in a way that makes them fit the criteria for integration and sign. The simplest approach to ensuring that the hole functions fulfil the requirements is to turn all the negative values of the exchange holes into zeros, and then truncating the exchange and correlation holes so that they integrate to -1 and 0, respectively.[3,37] By doing this one arrives at GGA XC functionals which have the general form

$$\begin{aligned} \mathrm{E}_{\mathrm{XC}}^{\mathrm{GGA}}[\rho_\alpha, \rho_\beta] &= \int f[\rho_\alpha(\vec{r}), \rho_\beta(\vec{r}), \nabla\rho_\alpha(\vec{r}), \nabla\rho_B(\vec{r})] d\vec{r} \\ \mathrm{E}_{\mathrm{XC}}^{\mathrm{GGA}}[\rho_\alpha, \rho_\beta] &= \mathrm{E}_{\mathrm{X}}^{\mathrm{GGA}}[\rho_\alpha, \rho_\beta] + \mathrm{E}_{\mathrm{C}}^{\mathrm{GGA}}[\rho_\alpha, \rho_\beta]. \end{aligned} \tag{30}$$

Due to the non-physical nature of the hole functions used in GGAs, the explicit forms of the exchange and correlation functionals tend to involve either semiempirical parameters or physically meaningless expressions. It is therefore compelling to only discuss these functionals on a qualitative level. Even though the GGA hole functions are not explicitly derived from theoretical physics, virtually all DFT used in chemistry utilizes GGA due to its ability to better represent molecular systems than the basic LDA. However, there are still problems with GGA and LDA functionals. Notably, the exchange-correlation potential at infinite distances does not decrease as the inverse of the distance ($-1/r$) as it should, but instead exponentially ($-e^{-r}$). This unphysical asymptotic behavior can be corrected by strictly enforcing the inverse rule at large distances, or partially by so-called hybrid functionals (See section 2.3.2). Not correcting the unphysical asymptotic behavior can lead to inaccuracies when predicting properties that depend on non-occupied orbitals, such as polarizabilities. At this point it should be mentioned

that practical XC functionals are evaluated based on their performance in replicating computational and experimental data—one of the most well-known such training sets is the G2 database,[38] which contains rigorous computational thermochemistry data on 55 small molecules.

Besides mitigating sources of inaccuracy in the GGA functionals, there is another intuitive way of developing more accurate functionals. Similar to how the LDA functionals were expanded to also consider the gradient of electron density, GGAs can be expanded to include the Laplacian of the density, in other words, the second spatial derivative, ∇^2. The functionals obtained this way are commonly called meta-generalized gradient approximations (meta-GGAs). Many of these meta-GGAs have shown promising results on the G2 benchmark,[39,40] but at the same time they tend to involve a plethora of empirical parameters, which can be argued to lead to a poor representation of the general performance. Despite the successes of meta-GGAs on the G2 benchmark, they hold a more niche position among currently available DFT functionals. The focus will now be shifted into other ways GGAs can be improved.

2.3.2 Global Hybrid Functionals

Before beginning the discussion of hybrid functionals, let us consider the separate exchange energy and correlation energy functionals in KS-DFT. Since the exact exchange[iii] term can be adopted from the HF approach, would it not be better to use it to calculate exchange exactly in DFT too? Indeed, this is possible by using the non-interacting reference system to calculate the exchange energy ($\widehat{H}_{\lambda=0}$ term in Eq. 21). However, this would lead to even greater problems than in the HF method, as the exchange and correlation holes would have different characteristics and therefore could not complement each other to correctly predict dissociation among other long-range effects. This is because the exact exchange and correlation holes are non-local, but the exact XC hole is local. In HF, the exchange hole is exact, but the correlation hole is missing, and in KS-DFT, both the exchange and correlation holes are local within the spin pair density, so mixing the correlation hole with the exact exchange hole leads to an unphysical, nonlocal XC hole. This is where the adiabatic connection from the previous chapter comes in: By approximating the integrand, E_{XC}^{λ}, in equation (22), one can define a global hybrid functional that combines the exact exchange energy of the non-interacting reference system with the approximate exchange and correlation energies of the fully interacting system, in arbitrary proportions. One of the simplest global hybrid functionals is the half-and-half (HH) functional[3,41]

[iii] Exchange is exact within the constraints of the wave function in the HF approach.

$$\mathrm{E_{XC}^{HH}} = \frac{1}{2}\mathrm{E_{XC}^{\lambda=0}} + \frac{1}{2}\mathrm{E_{XC}^{\lambda=1}}, \tag{31}$$

where the LDA exchange-correlation functional is used for the $\mathrm{E_{XC}^{\lambda=1}}$ term. The HH functional is derived from the approximation that $\mathrm{E_{XC}^{\lambda}}$ depends linearly on λ in the adiabatic connection (Eq. 22). By approximating the integral in the adiabatic connection, and thus the coupling strength integrated exchange-correlation hole (Eq. 26), kinetic correlation energy is included in this model. The reason why only using exact HF exchange in DFT may not be optimal also becomes apparent shortly.

Intuitively, the half-and-half exchange-correlation functional is far from reality in most molecules, but it was meant as more of a proof-of-concept functional, and better approximations soon followed.[42,43] There are many advantages in using hybrid functionals that arise from the higher level of theory, which have led to them being some of the more popular functionals in DFT for chemists. What makes global hybrid functionals and GGA functionals in general so versatile is the possibility of combining any proposed exchange functional with any correlation functional. Additionally, the inclusion of exact exchange changes the asymptotic behavior of the XC potential to a more physical, but still inaccurate form $-a/r$.

One of the functionals that followed the half-and-half functional was the B3PW91 functional.[41] It expanded the idea of the HH functional by employing established exchange and correlation functionals, and semiempirical coefficients to weigh the exact and approximate exchange portions, and correlation. The B3PW91 functional has the form

$$\mathrm{E_{XC}^{B3}} = \mathrm{E_{XC}^{LSDA}} + a\left(\mathrm{E_{XC}^{\lambda=0}} - \mathrm{E_{X}^{LSDA}}\right) + b\mathrm{E_{X}^{B}} + c\mathrm{E_{C}^{PW91}}, \tag{32}$$

where a represents the ratio of exact exchange to the total exchange, b and c weigh the gradient-corrected exchange and correlation functionals B[44] and PW91.[37] The coefficients a, b and c were chosen so that they reproduce some of the G2 thermodynamic data with the highest average accuracy. The coefficients optimized this way are $a = 0.20$, $b = 0.72$ and $c = 0.81$. Evaluated against some of the G2 data, the accuracy of B3PW91 exceeded many of alternative DFT methods available at the time. In comparison to the HH functional and some of the GGA functionals, the average error of the B3 functional is less than half, relative to G2 data. Even though B3 was optimized using this dataset, the results are still indicative of the viability of global hybrid functionals, and they give some information on the λ-dependence of $\mathrm{E_{XC}^{\lambda}}$ and the corresponding hole functional. Because the ratio of exact exchange to the total exchange is around 0.2, the integrals from equations (22) and (26) are closer to the values of the functionals at $\lambda = 1$. Therefore, it is reasonable to assume that the slope of these functionals is large and negative at $\lambda = 0$.

One of the most successful and popular global hybrid functionals has been the B3LYP exchange-correlation functional.[41,44–46] It is largely based on the B3PW91 functional, with the exception that the PW91 correlation functional is replaced with the LYP[45] functional. B3LYP has the form

$$\mathrm{E_{XC}^{B3LYP}} = (1-a)\mathrm{E_X^{LSDA}} + a\mathrm{E_{XC}^{\lambda=0}} + b\mathrm{E_X^{B88}} + c\mathrm{E_C^{LYP}} + (1-c)\mathrm{E_C^{LSDA}}, \qquad (33)$$

where a again denotes the ratio of exact exchange, and b and c represent the amounts of gradient-corrected exchange and correlation, respectively. The values for parameters a, b and c were adopted from the B3PW91 functional. This way the B3LYP functional would reach the same accuracy as B3PW91 for the G2 set. However, the reason behind the widespread success of B3LYP lies in that it performed well with various molecules, including systems that were previously troublesome for DFT, such as transition metal complexes and other open-shell systems. Another explanation for the popularity of B3LYP has to do with the inclusion of the LYP functional in popular quantum chemistry software at the time PW91 was developed, which is one of the reasons for the same empirical parameters in both B3PW91 and B3LYP.

In addition to semiempirical functionals such as the popular B3LYP, hybrid functionals have been developed without the use of empirical parameters. Instead, the amount of exact exchange is derived from theory. One such functional that does not involve semiempirical parameters is the PBE0 functional[36,43,47,48] (sometimes called PBE1PBE)

$$\mathrm{E_{XC}^{PBE0}} = \mathrm{E_{XC}^{PBE}} + a(\mathrm{E_X^{\lambda=0}} - \mathrm{E_X^{PBE}}), \qquad (34)$$

where the ratio of exact exchange to total exchange, a, is set to 25% as suggested by reasonings based on perturbation theory. While the PBE0 functional is competitive with other, semiempirical hybrid functionals, it is still susceptible to some inaccuracies linked to the HF theory like any hybrid functional. One of the most obvious drawbacks with global hybrid functionals has to do with the effects of exact exchange. By introducing any amount of exact exchange, the dissociation of electrons at long distances is disrupted, which causes all global hybrid functionals to be quite sensitive to the system. Nevertheless, global hybrid functionals have become an essential part among modern density functional methods thanks to their ability to reproduce experimental and reliable computational data to a high degree of accuracy.

2.3.3 Range-Separated Hybrid Functionals

While the hybrid functionals mentioned so far generally perform well, they still have problems involving the exact exchange at long distances not being eliminated by the Coulomb hole. To counteract this, it is possible to split the coulombic electron-electron interaction term in the exchange functional, resulting in a range-separated hybrid (RSH) functional. This is usually done by with the help of the relatively simple and well-behaved standard error function

$$\mathrm{erf}(x) = \frac{2}{\sqrt{\pi}} \int_0^x e^{-t^2} dt. \quad (35)$$

The Coulomb operator in the exchange functional is then written as

$$\frac{1}{r} = \frac{1 - \mathrm{erf}(\omega r)}{r} + \frac{\mathrm{erf}(\omega r)}{r}, \quad (36)$$

where r is the distance between two electrons, and ω is a so-called range-separation parameter.[3] This allows one to separate the ranges at which the different types of exchange in a hybrid functional apply, by choosing the range-separation parameter ω. By using equation (36) to write the $1/r$ term in exchange functionals, one obtains

$$\mathrm{E_X} = \mathrm{E_X^{SR}}(\omega) + \mathrm{E_X^{LR}}(\omega), \quad (37)$$

where $\mathrm{E_X^{SR}}(\omega)$ and $\mathrm{E_X^{LR}}(\omega)$ denote short-range and long-range exchange, respectively. Both are dependent on the range-separation parameter ω so that short-range exchange is negligible at large r, and vice versa. From equation (37) one can derive the general form of a RSH XC functional

$$\begin{aligned} \mathrm{E_{XC}^{RSH}} &= a\mathrm{E_X^{SR,\lambda=0}}(\omega) + (1-a)\mathrm{E_X^{SR,DFT}}(\omega) \\ &+ b\mathrm{E_X^{LR,\lambda=0}}(\omega) + (1-b)\mathrm{E_X^{LR,DFT}}(\omega) + \mathrm{E_C^{DFT}}, \end{aligned} \quad (38)$$

where a and b are parameters ranging from 0 to 1, $\mathrm{E_X^{\lambda=0}}$ is the exact exchange functional corresponding to the HF exchange, and $\mathrm{E_X^{DFT}}$ and $\mathrm{E_C^{DFT}}$ are approximate exchange and correlation functionals, respectively, that are used in DFT. There are also other methods for separating the functionals than using the error function, where the transition between ranges is not as smooth, but the error function serves as a simple example that is still used in some RSH functionals. Additionally, the separation is not strictly restricted to the exchange functional, and there have been experiments where the correlation functional is also separated.[49] The benefit of range-separation is the further increase in control over the exact exchange, and the ability to better simulate long-range exchange in hybrid functionals. This can be done by restricting the exact portion of the exchange to the long-range region so that the correct asymptotic behavior emerges, while calculating the short-range exchange approximately to preserve the DFT model.

One of the most popular range-separated hybrid functionals is the LC-ωPBE functional.[50–52] It is built from the short-range PBE[36] component and the long-range HF component. Contrary to many of its competitors, LC-ωPBE has only one semiempirical parameter—the range-separation constant ω. Yet it performs exceptionally on the G2 test against many other functionals that have multiple semiempirical parameters. LC-ωPBE has the formula

$$\mathrm{E_{XC}^{LC-\omega PBE}} = \mathrm{E_X^{SR-PBE}}(\omega) + \mathrm{E_X^{LR-HF}}(\omega) + \mathrm{E_C^{PBE}}, \quad (39)$$

where $\mathrm{E_X^{SR-PBE}}(\omega)$ and $\mathrm{E_X^{LR-HF}}(\omega)$ are the short-range PBE exchange and the long-range exact exchange, respectively. From the deceptively simple general form of equation (39), one might

wonder how such a simple functional can be competitive with other hybrid functionals. It is argued that the correct asymptotical behavior arising from the exact exchange at long distances is one of the reasons behind the success of LC-ωPBE. The advantages of LC-ωPBE include effects that it can accurately predict due to the long-range correction, such as difficult dissociation cases, polarizabilities of long chains and repulsive van der Waals potentials.

As an additional example of range separation in functionals, the Coulomb attenuation method (CAM) has been implemented to enable more control over the long- or short-range behavior of RSH functionals. CAM achieves this by including both contributions to exchange, HF and DFT, at any inter-electronic distance r. In the CAM-B3LYP[53] hybrid XC functional, this is done by adding two additional parameters to the range separation, which transforms equation (36) into

$$\frac{1}{r} = \frac{1 - (\alpha + \beta \operatorname{erf}(\omega r))}{r} + \frac{\alpha + \beta \operatorname{erf}(\omega r)}{r}, \tag{40}$$

where α and β are the additional parameters. These parameters enable the inclusion of a portion of HF exchange near $r = 0$ and a portion of DFT exchange up to $r \to \infty$, which was not possible with, for instance, the LC-ωPBE functional, in which the Fermi hole is integrated analytically using the range-separated Coulomb potential. In CAM, the range separation instead only applies to the LSDA portion of the Fermi hole. The authors then applied this form of range separation to a variety of trial functionals, among which the most consistent results were obtained with the B3LYP functional, with range-separation parameters $\alpha = 0.19$, $\alpha + \beta = 0.65$ and $\omega = 0.33$. The authors also showed how this method can provide accurate estimates on charge-transfer energies in addition to the more standard quantities used for evaluation of functionals.

2.4 Basis Sets

Up to this point the discussion has focused on the theory of density functional theory without considering how the wave functions and electron density are built for computational purposes. The aim of this chapter is to elucidate the ways in which the KS equations (Eq. 19) can be formatted into matrix equations using linear algebra, and what kinds of methods are used to constrict the amount of necessary computation.

Recall from chapter 2.2 that the energies of the KS orbitals are given by the KS equations (Eq. 19), which can be solved in a self-consistent way to produce the ground state electron density. So far, an explanation has not been given on how this is done in practice. The most obvious method would be to solve the KS equations numerically, which is indeed possible, but not practical. The explicit forms of the equations (Eq. 19) contain both differential and integral

terms for which modern computers are not optimized. Instead, it would be more reasonable to somehow convert the Kohn–Sham equations into something that can be expressed mostly with algebraic terms. Fortunately, there were computational schemes developed for this purpose in the HF method[3,54] that were later adopted to be used in DFT as well.

In order to simplify the KS equations, first the KS orbitals are defined as expansions of basis functions

$$\phi_i = \sum_{\mu}^{L} c_{\mu i}\eta_\mu, \tag{41}$$

where η_μ are simple basis functions weighed by expansion coefficients $c_{\mu i}$. Exact orbitals demand that all possible orbitals are used ($L = \infty$), but in practical use L is finite, which introduces another approximation. In quantum chemistry, HF theory with an infinite basis $L = \infty$ is known as the Hartree–Fock limit. Equation (41) describes a linear combination of atomic orbitals (LCAO) scheme, which gets its name from molecular orbital (MO) theory.[3,11] In DFT however, the basis functions η_μ do not necessarily represent atomic orbitals but instead can be approximated so that they are easier to compute but have important characteristics of the true orbitals. By substituting equation (41) into the KS equations, multiplying either side by a basis function η_γ, and integrating both sides over all space, one can rewrite the KS equations as

$$\sum_{\mu=1}^{L} c_{\mu i} \int \eta_\gamma \hat{\mathrm{f}}_{\mathrm{KS}} \eta_\mu d\tau = \varepsilon_i \sum_{\mu=1}^{L} c_{\mu i} \int \eta_\gamma \eta_\mu d\tau, \tag{42}$$

which can be separated into matrices

$$F^{\mathrm{KS}} C = SCE, \tag{43}$$

where the individual matrices are defined as

$$\begin{aligned} F_{\mu\gamma}^{\mathrm{KS}} &= \int \eta_\gamma \hat{\mathrm{f}}_{\mathrm{KS}} \eta_\mu d\tau\,, \\ C &= \begin{bmatrix} c_{11} & \cdots & c_{1L} \\ \vdots & \ddots & \vdots \\ c_{L1} & \cdots & c_{LL} \end{bmatrix}, \\ S_{\mu\gamma} &= \int \eta_\gamma \eta_\mu d\tau\,, \\ E &= \begin{bmatrix} \varepsilon_1 & \cdots & 0 \\ \vdots & \ddots & \vdots \\ 0 & \cdots & \varepsilon_L \end{bmatrix}, \end{aligned} \tag{44}$$

where $F_{\mu\gamma}^{\mathrm{KS}}$ is the Kohn–Sham matrix, C is a matrix containing the expansion coefficients $c_{\mu i}$, $S_{\mu\gamma}$ is an overlap matrix, and E is a diagonal matrix of the KS orbital energies. In this arrangement, the numerical method for finding the orbital energies has been transformed from the derivative and integral containing KS equations into a completely linear system of equations

by using linear algebra, which enables the efficient computation of the KS equations. It should be mentioned that the KS operator $\hat{f}_{KS}$ within the KS matrix includes functionals that depend on electron density which must now be expressed using the expanded KS orbitals as

$$\rho(\vec{r}) = \sum_{i}^{N} |\phi_i(\vec{r})|^2 = \sum_{i}^{N} \sum_{\mu}^{L} \sum_{\gamma}^{L} c_{\mu i} c_{\gamma i} \eta_\mu(\vec{r}) \eta_\gamma(\vec{r}), \quad \textbf{(45)}$$

where N is the number of electrons and L is again the number of basis functions per orbital. The expansion coefficients $c_{\mu i} c_{\gamma i}$ in the density function include all required information to construct the density when the basis functions are known, which is why they are often separated from the rest to skip unnecessary steps in computation.

All the basis functions used in constructing the HF or KS orbitals constitute a basis set. The properties of the basis set therefore include the formula for the basis function, and the size of the set. The choice of the basis function is of paramount importance as it directly affects the results of the computation. Likewise, if the basis set is too small, it may incorrectly lead to a situation where the orbitals behave inaccurately, notably omitting contributions from higher angular momentum quantum numbers that account for polarizability. One of the first basis sets comes from the atomic orbitals of a hydrogen atom, for which exact functions are available. These basis sets are called Slater-type orbitals[3] (STOs) and they have the general form

$$\eta^{\mathrm{STO}} = N\, r^{n-1}\, e^{-\zeta r}\, Y_{lm}(\theta, \phi), \quad \textbf{(46)}$$

where N is a normalization factor, n is the principal quantum number, ζ is an orbital exponent that defines how diffuse the orbital is, and $Y_{lm}(\theta, \phi)$ includes the spherical harmonics that define the shape of orbitals (*s*, *p*, *d*, *f*). STO basis sets are some of the most accurate representations available, but they have a major drawback in that the integrals in the KS matrix cannot be solved analytically, which increases computational cost and introduces another source of approximation. The approximation in question arises from the finite integration grid. In essence, when the integrals are calculated numerically, the values are computed separately in each volume element, and then summed to give the value of the integral. The smaller these volume elements are, or in other words, the finer the grid, the better the accuracy.

One of the simplest basis sets in called the Gaussian-type orbital (GTO) basis set.[3] Instead of deriving the set from physics as with the STO basis set, GTOs are composed of Gaussian functions, which simplifies the Coulomb integrals between orbitals. This approach allows the integrals in the KS matrix to be computed analytically, which is the main motivation behind GTOs. GTOs have the general form

$$\eta^{\mathrm{GTO}} = N\, x^l\, y^m\, z^n\, e^{-\alpha r^2}, \quad \textbf{(47)}$$

where l, m and n are defined as constituents of the angular momentum $L = l + m + n$, and α is the orbital exponent. This description of the wave-function lacks certain properties that atomic orbitals have: The derivative of each basis function is continuous when there should be a discontinuity at $r = 0$, the asymptotic behavior differs in that the GTOs decay too quickly, the basis functions are not orthogonal, and $L = l + m + n$ cannot be interpreted as angular momentum because the cartesian GTOs form a reducible basis for rotation elements.

Some of the deficiencies of Gaussian-type orbitals can be mitigated by using what are known as contracted Gaussian functions (CGFs).[3] These basis functions consist of linear combinations of GTOs, which allows them to match STOs and physical orbitals more accurately. The coefficients in the linear combination are predetermined to suit the basis set. While CGFs do not fully eliminate the problems regarding the unphysical properties of the GTOs, they can manage them better, with the price of added computation. Because of the exact nature of the integrals, CGFs are a popular choice for KS-DFT. While GTOs are the most used type of basis sets in quantum chemistry, other types of bases still exist.

In addition to analytic bases such as STO and GTO, it is possible to define the basis set in a purely numerical way by solving the KS equations for atomic orbitals. If the KS equations are solved numerically, a numerical basis set automatically emerges.[3] This process can be done with any XC functional, and when the same functional is used for both the DFT calculation and generating the basis set, the atomic orbitals have exact energies at the level of the functional.

As mentioned, the basis sets also contain the information about the amount of basis functions, and thus what atomic orbitals and molecular orbitals are modelled, regardless of what type of basis sets are used. At the simplest level, so-called minimal basis sets include only one basis function or contracted basis function for each atomic orbital, up to the valence shell. The most well-known minimal basis sets are the STO-*n*G basis sets,[55] in which *n* is the amount of Gaussian basis functions used to approximate the Slater-type orbitals. Minimal basis sets are insufficient when more than qualitative results are wanted. The minimal basis sets can be augmented by not only describing each atomic orbital by one basis function, but multiple basis functions.[3] In double-ζ (DZ) basis sets, each valence orbital is represented by a combination of two basis functions while the inner orbitals are described with single contracted basis functions, giving more freedom to each valence orbital. Triple- ζ (TZ) and quadruple- ζ (QZ) basis sets are also commonly used, and this approach can be continued to arbitrary large basis sets. Additionally, it is often useful to define polarization- and diffuse functions. Polarization functions add contributions from higher angular momentum orbitals to the atomic orbitals represented by basis functions, allowing them to ‘stretch’ and ‘bend’ anisotropically. This is particularly useful for modelling polarity and intricate bonds. Diffuse functions modify the

long-range behavior of the orbitals and can be important for modelling intermolecular interactions. Basis sets in which the valence shell is defined differently from other orbitals are called split valence (SV) basis sets, which is justified with the chemistry of atoms being mostly concerned of the valence shell electron structure.

As another example, the popular def2-branch[56] of GTO basis sets have been derived from the default bases used in the early versions of the quantum chemistry software TURBOMOLE,[57] utilizing relatively small pseudopotentials for heavy atoms, meaning that more electrons are included than in previous basis sets. The basis sets have been optimized to replicate experimental data on more than 300 molecules to a high degree of accuracy, based on various computational methods and different sizes of the basis set. By doing this, the performance of the basis set throughout a wide range of molecules was ensured, which has led to the def2-branch being a popular choice in DFT calculations and wave function-based methods alike.

2.4.1 Pseudopotentials

With large atoms it is sometimes beneficial to define the basis set so that some core-shell electrons are excluded, and the potential around the nucleus is altered. This way, the chemically insignificant inner-most electrons can be modelled approximately while the computational complexity is reduced. These approximations are called pseudopotentials or effective core potentials (ECPs). Pseudopotentials are so widely used in quantum chemistry calculations that it has become common practice to call calculations involving heavy elements without pseudopotentials all-electron calculations, although all-electron calculations have been gaining popularity recently.[3,11]

Pseudopotentials are often tied to basis sets, which in turn are described separately for different atoms. Notably, well performing pseudopotentials and basis sets for 3rd to 5th row elements were developed by Stevens and coworkers,[58] and similarly for lanthanides by Cundari and Stevens.[59] Especially for lanthanides and some of the heavier transition metals, the Stevens and Cundari–Stevens (CS) basis sets can provide a significant boost in the computation time. Another example is the Stuttgart pseudopotential included in the def2 basis sets, in which the pseudopotentials have been optimized to best replicate data from all-electron calculations.[60,61] Also, pseudopotentials can include relativistic effects which may be helpful in modelling certain quantities of heavy atoms. As will become apparent in section 4.2.1, the CS basis set has also proven to be quite useful in terms of the accuracy of DFT when calculating exchange coupling.

2.4.2 Relativistic Effects

In heavy atoms, the coulomb interactions between the inner electrons and the nuclei are stronger compared to lighter atoms, which means that they also move faster. This may pose problems when the electrons approach the speed of light, as Newtonian mechanics breaks apart due to special relativity.[3] These so-called relativistic effects include the Darwin term which involves electron-positron pair formation due to strong potentials in s-orbitals near nuclei, the often-dominant mass-velocity term that introduces an additional mass to any particle moving relative to a reference space, and a spin-orbit coupling term.[62] As a result of these relativistic effects not being included by default in the time-independent Schrödinger equation, different methods have been developed in quantum chemistry approaches to account for effects caused by the relativity of the motion of electrons around nuclei.

One strategy for incorporating these relativistic effects into quantum chemistry calculations is via altering the one-electron operators in the relativistic, Dirac Hamiltonian. The Dirac Hamiltonian is often represented as a matrix of coupled differential equations, from which the desired relativistic terms can be separated with various methods. Notable such approaches include the Douglas–Kroll–Hess methods (DKH),[63] or the zeroth-order regular approximation (ZORA).[3,62–64] DKH theory provides a way for systematically increasing the accuracy of relativistic effects. In DKH theory, the Dirac matrix elements are decoupled by multiplying the matrix with unitary matrices. In other words, the dependence of the differential equations on each other's variables is negated by multiplying the Dirac matrix by certain matrices and then multiplying the inverse of these matrices by the transformed matrix. After decoupling, the unphysical negative-energy elements can simply be ignored, which leaves the correct relativistic terms. The number of these unitary matrices denotes the order of the DKH method, with higher orders providing increasing accuracy. DKH of the second order is the most used level of DKH in quantum chemistry calculations. On the contrary to transformation techniques such as DKH, ZORA is an example of elimination techniques which aim to write the desired relativistic terms without the negative energy terms, by eliminating certain terms from the Hamiltonian. The remaining portion of the Hamiltonian contains an expression that is expanded into a power series, from which ZORA is approximated as only the first term of the expansion. Elimination techniques tend to have a lower computational cost but simultaneously they have problems involving the coupling of the matrix elements.

Alternatively, relativistic effects can be approximated in pseudopotentials, such as in the Stevens pseudopotentials[58] or the CS pseudopotentials for lanthanides.[59] In the case of the CS pseudopotentials, they are derived from calculations with the relativity-adjusted one-electron (Dirac) Hamiltonians. The resulting orbitals from these so-called Dirac–Hartree–Fock (DHF)

calculations are converted to nodeless entities, which can then be averaged to yield a numerical relativistic pseudopotential. The numerical pseudopotential can then be approximated in an analytic form by optimizing the analytic expression to match the numerical potential as closely as possible.

2.5 Dispersion Correction Methods

Weak interactions between molecules are typically explained by electric dipole moments arising from the relative positions of electrons and nuclei in the molecules. These dipolar forces can either originate from permanent electric dipole moments, which leads to a dipolar bond, or from mutual polarizabilities of two molecules, which manifest as the attractive forces commonly known as dispersion or London forces.[65] The polarizabilities represent mixing of virtual charge transfer states with the ground state, which results in a weak dipolar interaction. Dispersion is considered to be an electron correlation effect, and thus, it is difficult to express in many quantum chemistry applications.[3,11]

In DFT, the exchange-correlation term is a functional of electron density, but dispersion occurs between distant electron densities, so it is not included in the equations shown previously.[3] This is because in all approximate functionals that have been mentioned, the electron density is mostly treated locally,[iv] in other words the density does not encode information related to other parts of the density. The sole exception to this is the universal functional proposed by Hohenberg and Kohn[1] which, by definition, includes all energy contributions in the exact Schrödinger equation.

To better model weakly-bound systems, so-called dispersion correction methods are employed. Some modern functionals include them by default, but there are dispersion correction methods that can be added onto existing functionals such as the B3LYP and PBE0 hybrid functionals or the LC-ωPBE range-separated hybrid functional. One of the most popular branches of such dispersion corrections consists of the DFT-D type methods.[66,67]

The DFT-D dispersion correction methods were designed to calculate dispersion energy separately from the DFT calculation. One of the newest among these dispersion corrections is the DFT-D3 method.[66] In DFT-D3, the dispersion energy consists of two- and three-body energy components

$$\mathrm{E_{DFT-D3}} = \mathrm{E_{KS-DFT}} - \mathrm{E_{disp}} = \mathrm{E_{KS-DFT}} - (\mathrm{E_2} + \mathrm{E_3}), \qquad (\mathbf{48})$$

where the two-body component dominates and is defined as

[iv] The possible non-local components include exact exchange in hybrid functionals, or gradient information which technically cannot be determined without the immediate surroundings of the reference point.

$$\mathrm{E}_2 = \sum_{AB} \sum_{n=6,8} s_n \frac{C_n^{AB}}{r_{AB}^n} f_{d,n}(r_{AB}), \quad (49)$$

where C_n^{AB} are optimized dispersion coefficients of order n for atom pairs AB, r_{AB} is the distance between atoms A and B, and s_n are global scaling factors which ensure correct asymptotic $1/r^6$ behavior. $f_{d,n}$ is a damping function which defines the range of the dispersion and, in the process, eliminates singularities and double counting of the dispersion. Equations (48) and (49) show that dispersion energy can be incorporated into DFT without further complications in the KS scheme. The drawback of this approach is that the dispersion energy is not included in the KS equations which results in yet another approximation to the method. Nevertheless, dispersion correction methods can be useful tools when accurate energies are wanted.

3 Magnetism and Exchange Coupling

Magnetism is a phenomenon that has been known for millennia, but its causes have only surfaced with modern electronic structure theories. It is now widely known that long-range magnetic ordering arises from exchange coupling. Exchange coupling refers to the alignment of electron spins that is caused by exchange interaction. It is a quantum mechanical phenomenon that relates to a variety of important phenomena in chemistry, notably covalent bonding and the Pauli principle. In this chapter, exchange coupling is discussed from different aspects including electronic structure, its role in magnetism, orbital symmetry considerations, and how exchange coupling constants can be extracted from computational data.

3.1 Theory of Electronic Structure and Magnetism

Exchange coupling is the main effect responsible for ferromagnetism, and other forms of permanent magnetism in materials due to long-range magnetic ordering, including antiferromagnetism and ferrimagnetism.[11] The mechanism behind exchange coupling is exchange interaction, a quantum mechanical phenomenon where the wave functions of identical fermions, particles with half-integer spin such as electrons, are antisymmetric relative to the exchange of their spatial and spin coordinates.[26] The discussion to follow focuses on the mathematics and physics of exchange interaction and how it manifests in nature as covalent bonding (according to some models), the Pauli exclusion principle, and notably ferromagnetism.

In theoretical chemistry and physics, covalent bonds have been explained using different models. In many theories, the underlying mathematics tells us that what we observe as covalent bonding arises from the notion that electrons are indistinguishable, in other words, identical under the exchange of their position. The combined wave function of two electrons in a simple diatomic molecule such as H_2 can be written as their product

$$\Psi = \psi_a(\vec{x}_1)\psi_b(\vec{x}_2), \tag{50}$$

where ψ_a and ψ_b are the wavefunctions of individual electrons, and $\vec{x}_i$ include their spatial and spin coordinates. However, this is not the whole picture. In this model, the wave functions of the electrons are independent of each other, but it can be said that when the electrons are close together, it is impossible to know which electron is which. Therefore, a more accurate description of the system would be a linear combination of the two possibilities

$$\Psi = \{n[\psi_a(\vec{r}_1)\psi_b(\vec{r}_2)] + m[\psi_a(\vec{r}_2)\psi_b(\vec{r}_1)]\}\sigma(s_1, s_2), \tag{51}$$

where n and m are constants, and $\sigma(s_1, s_2)$ is the spin function which is here separated from the wave functions. This is the description of a covalent bond in a model called valence-bond (VB) theory.[11] By closer examination of equation (51), it can be seen that the two-electron wave functions that form the total wave function have their coordinates exchanged. When the one-electron wave functions interfere constructively and the total wave function is normalized, the resulting total wave function has a lower energy than either of the separate wave functions. It is important to note that equation (51) only holds when the spin components of the coordinates of the individual electrons are opposite, as mandated by the antisymmetry of the two-electron wave function Ψ under the exchange of the individual electrons' spatial and spin coordinates $\sigma(s_1, s_2) = -\sigma(s_2, s_1)$. In conclusion, VB theory provides an intuitive model for covalent bonds arising from the exchange of two electrons that are near each other in space, and correctly predicts the Pauli exclusion principle when spins are included and the antisymmetry of the wave function is assumed. However, it has in many ways been surpassed by molecular orbital theory, in which the orthogonality of molecular orbitals eases the calculation of larger wave functions.

In molecular orbital (MO) theory, electronic structures can be constructed from approximate molecular orbitals which are linear combinations of atomic orbitals (LCAOs)

$$\phi = c_A\chi_A + c_B\chi_B, \tag{52}$$

where χ_A and χ_B are wave functions of atomic orbitals A and B, respectively, and c_A and c_B are constants. The key difference to VB theory is that the combining atomic orbitals do not have to be occupied, and electrons are not localized to bonds.[11] Instead, the electrons are spread throughout the molecule by filling the molecular orbitals in order, starting from the MO with the lowest energy. In diatomic molecules, the molecular orbitals are created in pairs of bonding and antibonding MOs. The bonding molecular orbitals are an analogue for covalent bonds, and

they result from the constructive interference of two atomic orbital wave functions. Conversely, in the antibonding MOs, the wave functions interfere destructively, resulting in a lower electron density in the internuclear space if the orbital is occupied. In larger molecules and in general, the molecular orbitals must be orthogonal, which does not necessarily mean that the orbitals are strictly bonding or antibonding. The theoretical basis for bonding in the MO theory has been attributed to the decrease in bonding orbital energy due to the increase in this internuclear electron density—higher density between the nuclei lowers the potential energy by allowing both nuclei to interact with more of the electron density in total. Similarly, in the antibonding orbital the energy is increased more relative to the individual atomic orbitals because electron density is pushed away from the nuclei outside of the intermolecular region, elevating the Coulomb potential both between the nuclei, and between nuclei and electrons.

In MO theory, covalent bonding does not strictly arise from the exchange of two electrons, but instead from the delocalization of electrons between nuclei, which is often approximated as LCAOs.[11] In the MO theory, exchange interaction appears because the expectation value for the Coulomb operator is taken from the fermionic wave function. Due to affecting the energy of the wave function, exchange interaction causes spins of individual electrons in different orbitals to be parallel because this minimizes the Coulomb repulsion between them, and between these types of orbitals the internuclear electron density is not affected, assuming that other types of interactions are sufficiently small. Therefore, MO theory can explain forms of magnetism like the well-known paramagnetism of O_2 in its triplet ground state due to the exchange interaction between electrons on degenerate orbitals. There is a key term in MO theory that is very useful our discussion on exchange coupling, that is, overlap integrals

$$S = \int \psi_A^* \psi_B \, d\tau, \tag{53}$$

where ψ_A and ψ_B are (atomic) orbitals, and integration is done over all space. The integrals measure how much two orbitals can interfere with each other. Consequently, they indicate how likely two orbitals form bonding and antibonding orbitals, in other words a covalent bond, but the integral does not indicate the Coulomb and exchange interactions that affect spin.

The antisymmetry of fermions over exchange has the consequence of proximate electrons, such as in covalent bonds, having to assume antiparallel spins, as was shown in VB theory and MO theory. This is known in literature as the Pauli exclusion principle. This effect is also important for the context of exchange coupling as will shortly be shown. It can also be derived from the antisymmetry of electrons over exchange without any other models. Consider two wave functions that represent electrons. These wave functions can be written as a total wave

function that is antisymmetric with respect to exchange of its variables, the spatial and spin variables of each electron

$$\Psi(\vec{x}_1, \vec{x}_2) = -\Psi(\vec{x}_2, \vec{x}_1), \quad (54)$$

where Ψ is the total wave function of two electrons with coordinates (space and spin) $\vec{x}_1$ and $\vec{x}_2$. If we now set both spins to be parallel and the spatial coordinates to be the same

$$\vec{x}_1 = \vec{x}_2, \quad (55)$$

and substitute $\vec{x}_2$ into equation (54), it becomes

$$\Psi(\vec{x}_1, \vec{x}_1) = -\Psi(\vec{x}_1, \vec{x}_1) = 0. \quad (56)$$

From this expression it is apparent that if two wave functions were to have the same spatial and spin coordinates, the total wave function would have to be zero, meaning that there is no wave function that can satisfy the condition. This derivation is independent of the total wave function Ψ so it shows that the Pauli principle is a fundamental condition that all two-electron wave functions must obey, as long as the elements are antisymmetric over exchange. The implications of the Pauli principle for exchange coupling involve the spins aligning antiparallel to each other, promoting antiferromagnetic coupling. This effect is prominent in systems where two orbitals with one electron each can combine to form a covalent bond. Because the electrons may now be considered to be on a new molecular orbital, as in they have the same spatial coordinate, Pauli exclusion principle tells us that their spins must be antiparallel to each other. This concept can be extended to intermolecular interactions, such as between two stable radicals or two transition metal complexes. In these types of systems, the partially filled orbital are called magnetic orbitals, and they are susceptible to dimerizing, in other words interacting covalently with other magnetic orbitals. For example between two stable radicals, the more covalent the bonding between two singly-occupied molecular orbitals (SOMOs) is, the more antiferromagnetic the exchange coupling between them tends to be.[12,68] This also applies for other magnetic orbitals, such as the partially occupied *d*-orbitals in transition metals.[69,70]

3.1.1 Magnetic Materials and Coupling

Now that electronic structures and the Pauli exclusion principle have been revisited from a theoretical point of view, it is time to continue the discussion of magnetism. The most common type of magnetism in molecules is diamagnetism. A diamagnetic substance is repelled by magnetic fields because of currents that are induced in the electron structure of the substance.[11] Typically, diamagnetic molecules act this way because all their electrons are paired and the molecules do not have an intrinsic magnetic moment. Thus, only the induction currents contribute to magnetism. These induction currents are present in all matter that contains electrons, but in paramagnetic substances, their innate magnetic moments overcome this effect.

In molecules, paramagnetism typically arises from unpaired electrons, although it is theoretically possible to excite most molecular systems to a paramagnetic state with extremely large magnetic fields. In bulk material, these molecular properties manifest as magnetism. Without the presence of an external field, the magnetic moments in paramagnetic substance align randomly due to temperature. In an external magnetic field, these magnetic moments tend to align with the field. Therefore, paramagnetic substances are categorized as strengthening the external magnetic field. A measure for these effects is magnetic susceptibility

$$M = \chi H \tag{57}$$

where χ is volume magnetic susceptibility, H is the magnetic field strength, and M is the magnetization defined as the average magnetic moment multiplied by the number density of molecules, and a magnetically isotropic substance is assumed. By definition, diamagnetic substances have $\chi < 0$ and paramagnetic substances $\chi > 0$. This quantity can be probed experimentally with good accuracy using a superconducting quantum interference device (SQUID). As mentioned, a paramagnetic substance only has magnetization in an external magnetic field, but there are categories for permanent magnetism.

Ferromagnetic solids contain large domains where magnetic moments align parallel with each other. This only happens below a certain temperature specific to each paramagnetic solid, called the Curie temperature.[11] There is also antiferromagnetism where the magnetic moments within domains align antiparallel and cancel each other out, and ferrimagnetism, where the moments only partially cancel out. These types of magnetism typically occur in metals and semiconductors, and thoroughly explaining them is outside of the scope of this thesis. However, it is important to make the distinction between ferromagnetic (FM) and antiferromagnetic (AFM) substances and ferromagnetic and antiferromagnetic couplings, even though the latter are often largely responsible for the magnetic properties of the material. In the context of magnetic coupling, FM and AFM coupling refer to whether two magnetic moments are coupled parallel or antiparallel, which albeit often are the mechanisms behind long-range magnetic ordering in the corresponding substances. For example, liquid oxygen is paramagnetic in its ground state, but the exchange coupling between its unpaired electrons is ferromagnetic.

3.1.2 Effects of Orbital Symmetry in Exchange Coupling

Molecular orbital theory grants us a way of modelling electronic structures based on molecular orbitals, which can be approximated as linear combinations of atomic orbitals. For exchange coupling, a particularly useful concept introduced along the MO theory is overlap integrals (Eq. 57). When the overlap integral between two orbitals is zero, it is said that the orbitals are orthogonal

$$S = \int \psi_A \psi_B \, d\tau = 0. \quad (\mathbf{58})$$

Orthogonal atomic orbitals cannot form molecular orbitals together because the added electron density in the region where the orbitals overlap is zero, and therefore it does not contribute to bonding. As such, the atomic orbitals of a single atom are orthogonal with each other,[71] and orthogonal atomic orbitals from different atoms do not form molecular orbitals together. The concept of orthogonality can also be applied to two molecular orbitals in different molecules, which becomes important when the orbitals are singly occupied, as will be shown later in this section. However, electrons on two orthogonal orbitals can still experience direct exchange interactions, in the form of reduced electron density in the region where the two densities would overlap, due to the alteration of the total wave function via exchange of two electrons with the same spin. Orbitals that do not form molecular orbitals are known in MO theory as non-bonding orbitals, and they are essentially orthogonal with every other orbital in the system.

In the scenario where two different molecular orbitals are not orthogonal, for example in π-π stacked systems, there often is a degree of covalency between the molecular orbitals, which leads to AFM coupling. However, if the π-π stacks are aligned so that the nodes of one orbital overlap with the peaks of the other, the orbitals can become orthogonal, which suppresses the covalency. This concept is called accidental orthogonality, and it can be achieved by chemical substitution although it is very difficult.[19,72] The benefit of achieving orthogonality between two proximate molecular orbitals is that the direct exchange is preserved while covalency is suppressed completely. If both molecular orbitals are occupied by a single electron, the coupling between them would only contain ferromagnetic contributions from the direct exchange. In addition to accidental orthogonality, it is possible to achieve orthogonality between two molecular orbitals with certain symmetry considerations.

Contrary to accidental orthogonality, strict orthogonality relies on the orthogonality imposed by different symmetries of the magnetic orbitals. It was realized that when the two orbitals transform as different irreducible representations of the same point group, their overlap integral must be zero so they are strictly orthogonal.[70] This concept was first introduced for transition metal complexes but it was later expanded to also cover organic radical-based molecules.[73] The strict orthogonality approach gives us a way of designing molecules that show intramolecular ferromagnetic coupling, and also provides valuable insight into how the antiferromagnetic and ferromagnetic contributions can be quantified in such systems.[69]

Exchange coupling consists of two contributions, the direct exchange of electrons promoting FM coupling, and the covalency arising from non-orthogonal orbitals promoting AFM coupling. It turns out that the description of a covalent bond in the valence bond theory became

a particularly effective starting point for investigating exchange coupling between electron spins.[74] The coupling between two magnetic centers A and B can be quantified as an exchange coupling constant

$$J = 2\beta S + K, \tag{59}$$

where S is the overlap integral (Eq. 57), β is the resonance integral defined as

$$\beta = \int \psi_A \hat{\mathrm{H}} \psi_B \, d\tau = \langle \psi_A | \hat{\mathrm{H}} | \psi_B \rangle, \tag{60}$$

and K is an exchange integral

$$K = \langle \psi_A \psi_B | r_{12}^{-1} | \psi_B \psi_A \rangle. \tag{61}$$

The signs of S and β are always opposite, so the first term in equation (58) is always negative and contributes to AFM coupling. On the contrary, the exchange integral always contributes to FM coupling, but it is much weaker than the AFM contribution. From equations (59–61) it becomes apparent that while both contributions depend on the proximity of the orbitals, only the AFM portion depends on the overlap integral. Therefore, ferromagnetic coupling typically only appears when the overlap integral is zero (strict orthogonality) or very small (accidental orthogonality). These effects can be related to energies of different electron configurations using the Heisenberg–Dirac–van Vleck (HDvV) Hamiltonian which is one of the foci of the next chapter.

3.2 Exchange Coupling in DFT

Density functional theory can be used to compute the energies of electron densities which correspond to electron structures. In UKS methods, spin is included in the KS orbitals, which enables the computation of energies for different spin multiplicities. When the energies of different configurations are known, it is possible to derive the coupling constants using different methods like the broken symmetry (BS) approaches derived from the HDvV[13,17,18] Hamiltonian

$$\hat{\mathrm{H}}_{\mathrm{HDvV}} = -2 \sum_{i<j} \sum_{j} J_{ij} \hat{S}_i \hat{S}_j, \tag{62}$$

where i and j denote all binary combinations of magnetic centers in the system (typically only from the unpaired electrons of atoms), J_{ij} is the exchange coupling constants between i and j, and $\hat{S}$ are the spin operators that return the spin from the electrons in the moieties that they operate on. One such broken symmetry approach is the Yamaguchi projection.[75–77]

The computed energies of low-spin states in radical systems sometimes involve considerable spin-contamination. This observation led to the development of several broken symmetry (BS) calculation schemes.[14–16] These calculations utilize the spin projection term to mitigate the effects of spin contamination from higher multiplicities. The most generalized of these BS

calculation methods is Yamaguchi projection,[75–77] as it applies regardless of how much the SOMOs overlap. Yamaguchi projection has the formula

$$J = E_s - E_t \approx 2\frac{E_{\mathrm{LS}} - E_{\mathrm{HS}}}{\langle S^2\rangle_{\mathrm{HS}} - \langle S^2\rangle_{\mathrm{LS}}}, \tag{63}$$

where E_s is the energy of the true singlet state (radical spins antiparallel), E_t is the energy of the true triplet state (spins parallel), and E_{HS}, E_{LS}, $\langle S^2_{\mathrm{HS}}\rangle$ and $\langle S^2_{\mathrm{LS}}\rangle$ are the energies and spin projection terms from computations such as unrestricted Kohn–Sham DFT. It should be mentioned that the $\langle S^2\rangle$ terms are better defined in the HF method, for which the Yamaguchi projection was initially developed for, but it can also be applied to KS-DFT. It should be noted that in the broken symmetry low-spin (LS) state, also called a BS-state, the α- and β-spins are strictly located at different magnetic centers, and in general BS refers to the separation of α- and β-spins to different magnetic centers.

Yamaguchi projection was generalized even further with the inclusion of geometry considerations.[78] Clearly, the optimized geometry depends on the spin state. Therefore, there will always be a discrepancy between reality and computations in the geometries of magnetically coupled systems. However, it is possible to adjust equation (63) so that it represents a system where its geometry can change between states (the adiabatic singlet-triplet gap). First, it is assumed that the high-spin (HS) and LS geometries are reasonably close to the true triplet and singlet geometries, respectively. Then, one can write the singlet energy as

$$\begin{aligned} E_s^s &= E_t^s + J^s \approx E_{\mathrm{LS}}^{\mathrm{LS}} = E_{\mathrm{HS}}^{\mathrm{LS}} + J^{\mathrm{LS}} \\ E_{\mathrm{LS}}^{\mathrm{LS}} &= E_{\mathrm{HS}}^{\mathrm{LS}} + 2\frac{E_{\mathrm{LS}}^{\mathrm{LS}} - E_{\mathrm{HS}}^{\mathrm{LS}}}{\langle S^2\rangle_{\mathrm{HS}}^{\mathrm{LS}} - \langle S^2\rangle_{\mathrm{LS}}^{\mathrm{LS}}}, \end{aligned} \tag{64}$$

where the superscripts denote the spin state used in computational geometry optimization, and subscripts indicate the spin state imposed after optimization. Using equation (63), one can finally define the adiabatic Yamaguchi projection

$$J_{\mathrm{adiabatic}} = E_{\mathrm{HS}}^{\mathrm{LS}} + 2\frac{E_{\mathrm{LS}}^{\mathrm{LS}} - E_{\mathrm{HS}}^{\mathrm{LS}}}{\langle S^2\rangle_{\mathrm{HS}}^{\mathrm{LS}} - \langle S^2\rangle_{\mathrm{LS}}^{\mathrm{LS}}} - E_{\mathrm{HS}}^{\mathrm{HS}} = E_{\mathrm{LS}}^{\mathrm{LS}} - E_{\mathrm{HS}}^{\mathrm{HS}}. \tag{65}$$

Out of all the energy terms in equation (65), only $E_{\mathrm{HS}}^{\mathrm{HS}}$ can be produced from a system that can be described as a single Slater determinant and is therefore more reliable than the LS states and geometries. Whenever LS state is optimized or its energy is calculated, the spin contamination from higher multiplicities tends to be present. The Yamaguchi projection solves part of this problem when calculating the coupling constants. However, the effects of spin contamination are still reflected on the geometry optimized in the LS state, hence the assumption of realistic geometries. Nevertheless, the adiabatic Yamaguchi projection is one of the most used methods for calculating coupling constants in radical-based systems based on computational data.

As an alternative method for Yamaguchi projection and other BS methods, the exchange couplings can be calculated from only the information about the DFT energies of different spin states. Once the energies of several electronic structures of a molecule have been calculated with DFT, the exchange coupling constants can be derived from them by working backwards from the HDvV Hamiltonian (Eq. 62).[13,79,80] For example, the spin operator of a radical molecule would return either +½ or -½, while the spin operator of a gadolinium atom would return $+7/2$ or $-7/2$ or anything between those values depending on its spin state, although only the maximum values are used in BS approaches. It should be noted that because the KS approach is based on a single determinant, it introduces another approximation to the model. As another limitation, this model is not applicable to ions with large spin-orbit coupling (See chapter 4). Also, the energies given by the HDvV Hamiltonian only account for the magnetic interactions, in other words the exchange coupling constants.

When the energies of the different spin configurations have been calculated, the corresponding exchange coupling constants can be obtained. For example, let us consider a molecule with two gadolinium ions and a bridging radical ligand, similar to a molecule reported by Long and coworkers (Fig. 1; a review of this molecule will be provided in section 4.2.3).[81] Assuming that the gadolinium atoms are in identical chemical environments and geometries, this type of molecule essentially has three candidates for the most stable spin multiplicity: First, all the spins can be parallel (HS). Second, the gadolinium spins can be antiparallel (LS), or third, the gadolinium spins can be parallel while the radical spin is antiparallel (intermediate-spin, IS). Each of these multiplicities corresponds to a coupling energy given by the HDvV Hamiltonian

$$\begin{aligned}
\hat{\mathrm{H}}_{\mathrm{HDvV}} &= -2\left(J_{\mathrm{Gd-R}}\hat{S}_{\mathrm{Gd}}\hat{S}_{\mathrm{R}} + J_{\mathrm{Gd'-R}}\hat{S}_{\mathrm{Gd'}}\hat{S}_{\mathrm{R}} + J_{\mathrm{Gd-Gd'}}\hat{S}_{\mathrm{Gd}}\hat{S}_{\mathrm{Gd'}}\right) \\
E_{\mathrm{HS}} &= -2\left(\frac{7}{4}J_{\mathrm{Gd-R}} + \frac{7}{4}J_{\mathrm{Gd'-R}} + \frac{49}{4}J_{\mathrm{Gd-Gd'}}\right) \\
E_{\mathrm{LS}} &= -2\left(\frac{7}{4}J_{\mathrm{Gd-R}} - \frac{7}{4}J_{\mathrm{Gd'-R}} - \frac{49}{4}J_{\mathrm{Gd-Gd'}}\right) \\
E_{\mathrm{IS}} &= -2\left(-\frac{7}{4}J_{\mathrm{Gd-R}} - \frac{7}{4}J_{\mathrm{Gd'-R}} + \frac{49}{4}J_{\mathrm{Gd-Gd'}}\right).
\end{aligned} \tag{66}$$

One can then consider these representations as a set of equations and solve it for each coupling constant, which gives

$$\begin{aligned}
J_{\mathrm{Gd-R}} &= -\frac{1}{7}(E_{\mathrm{HS}} + E_{\mathrm{LS}}) \\
J_{\mathrm{Gd'-R}} &= \frac{1}{7}(E_{\mathrm{LS}} + E_{\mathrm{IS}}) \\
J_{\mathrm{Gd-Gd'}} &= -\frac{1}{49}(E_{\mathrm{HS}} + E_{\mathrm{IS}}).
\end{aligned} \tag{67}$$

However, the DFT energies contain not only the exchange coupling energy but also every other energy contribution in the calculation that does not depend on the multiplicity

$$E_{\mathrm{DFT}} = E_0 + E_{\mathrm{HDvV}}. \tag{68}$$

Therefore, equation (67) does not suffice for calculating exchange coupling constants directly from the DFT energies. Instead, it must be formatted in a way where the unknown E_0 terms vanish

$$\begin{aligned} \hat{\mathrm{H}}_{\mathrm{HDvV}}\psi &= (E_{\mathrm{DFT}} - E_0)\psi \\ (\hat{\mathrm{H}}_{\mathrm{HS}} - \hat{\mathrm{H}}_{\mathrm{LS}})\psi &= \left(E_{\mathrm{DFT,HS}} - E_{\mathrm{DFT,LS}}\right)\psi. \end{aligned} \tag{69}$$

This gives

$$\begin{aligned} J_{\mathrm{Gd-R}} + J_{\mathrm{Gd'-R}} &= \frac{1}{7}(E_{\mathrm{IS}} - E_{\mathrm{HS}}) \\ J_{\mathrm{Gd'-R}} + 7J_{\mathrm{Gd-Gd'}} &= \frac{1}{7}(E_{\mathrm{LS}} - E_{\mathrm{HS}}) \\ J_{\mathrm{Gd-R}} - 7J_{\mathrm{Gd-Gd'}} &= \frac{1}{7}(E_{\mathrm{IS}} - E_{\mathrm{LS}}). \end{aligned} \tag{70}$$

In this example, the gadolinium atoms were assumed to be in equivalent chemical environments, which means that one can write

$$J_{\mathrm{Gd-R}} = J_{\mathrm{Gd'-R}}, \tag{71}$$

and thus, solve equation (70) for the coupling constants J_{i}. If the geometries and chemical environments near the gadolinium atoms were different, there would be a fourth spin state that would need to be solved—a LS state where the spins of the gadolinium atoms were swapped. In this example, these states are equivalent, and we can substitute equation (71) into equation (70), which gives

$$\begin{aligned} J_{\mathrm{Gd-R}} = J_{\mathrm{Gd'-R}} &= \frac{1}{14}(E_{\mathrm{IS}} - E_{\mathrm{HS}}) \\ J_{\mathrm{Gd-Gd'}} &= \frac{1}{98}(2E_{\mathrm{LS}} - E_{\mathrm{HS}} - E_{\mathrm{IS}}). \end{aligned} \tag{72}$$

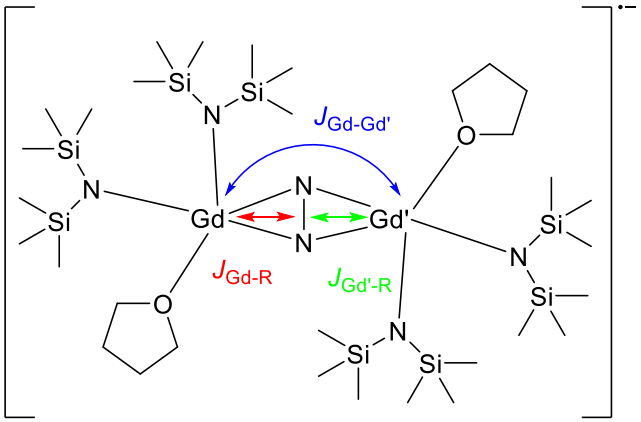

Figure 1. The exchange coupling constants in the Gd-dimer reported by Long *et al.*.[81] The coloured double-arrows represent the intramolecular exchange couplings. The unpaired electron in N_2^{3-} is delocalized between the nitrogen atoms, on a π*-orbital.

This was an example of the use of the HDvV Hamiltonian in conjunction with DFT calculations to estimate the coupling in a radical bridged gadolinium dimer. The method shown here is in theory applicable to any type of system with multiple magnetic centers. However, it cannot be stressed enough that KS-DFT is a single determinant method, and thus cannot fully represent excited magnetic states, which can sometimes lead to significant errors in practice, although very accurate coupling constants can be obtained. This approach is somewhat less accurate than the other reviewed BS methods due to the isotropic magnetic moment approximation and not accounting for spin contamination, but its advantage lies in the applicability to a wider range of systems.

4 DFT and Molecular Magnetism

In general, molecular magnetism covers various forms of magnetism that arise from molecular structures.[19] Molecular magnetism started with research on transition metal clusters that exhibited interesting magnetic properties,[69,70] and the field has expanded to also cover lanthanide complexes, and to some degree radical-based materials. Some of the transition metal clusters and lanthanide-based systems can be single-molecule magnets (SMMs) that are classified as molecules that can display magnetic hysteresis below a so-called blocking temperature. One of the main topics of the field today is the development of SMMs. The early half of this chapter discusses the theory in the field on a qualitative level, while the latter half reviews instances in which DFT has been used in literature to gather information on the magnetic properties of molecules.

4.1 Molecular Magnetism

Magnetism is a phenomenon that has been known for millennia, but its origins have remained elusive until the discovery of electron spin and angular momentum in the 20th century. As explored in section 3.1, magnetism arises from the angular momenta of charged particles and the spins of particles. The broad field of molecular magnetism involves the design, synthesis, and exploration of magnetic properties of magnetic materials and molecules. An interesting topic related to molecular magnetism came along organic, radical-based conductive materials in the late 1900s, when researchers started wondering if room-temperature organic ferromagnets were possible to synthesize. So far this goal of organic ferromagnets has not yet been reached, but alternative, for instance, transition-metal based molecular materials have been proposed. In fact, some of the earliest contributions in the field included materials consisting of manganese clusters.[19,82] Later, the properties of these clusters were implemented into molecules containing only single transition metal ions.[83] It was also realized that lanthanides could perform even better in these so-called SMMs.[84,85]

The quest for organic ferromagnets has been a long and difficult one. However, several key discoveries have been made throughout the efforts. For instance, the principle of orbital symmetry in leading to ferromagnetic coupling is one such discovery. One might ask why ferromagnetic radical materials have not yet been realized if ferromagnetic coupling between radicals has been demonstrated. The answer lies in the three-dimensional structure of the material: Even though the radicals can be arranged in ways in which they exhibit ferromagnetic coupling, this is often limited to linear structures, as it is difficult to extend the ferromagnetic coupling of radicals to occur between chains, in other words the coupling seen in π–π stacks and other types of linear assemblies seldom expands beyond the linear structure, even if the material is three-dimensional. These interactions between neighboring molecules in a chain are not enough to overcome the thermal mixing of magnetic states in all but the lowest temperatures.[19] Instead, even the best-performing systems relax to an equilibrium after some time. This is a common theme in lower-dimensional magnetic materials.

In addition to bulk magnetic materials, smaller-dimensional assemblies have been investigated. Notably, the zero-dimensional structures that can act as SMMs. These structures can range from clusters containing multiple magnetic centers to single-ion magnets, which only contain one magnetic ion. There are many benefits with this approach. First, clusters and smaller structures can be crystallized, dissolved, and dispersed on surfaces, and in general manipulated in various ways. Second, it is easier to design the chemical environment of ions in small assemblies, providing easier avenues for controlling the magnetic behavior.

Single-molecule magnets are defined as molecules that express magnetic hysteresis that originates from within the molecule itself. This phenomenon is dynamic in the sense that it is dependent on the temperature. However, most molecules do not show this behavior even very close to absolute zero. Therefore, it is convenient to say that any molecule that is capable of magnetic hysteresis is a SMM and shows SMM behavior under a blocking temperature. Typical components of SMMs are specific transition metal and lanthanide ions due to their high intrinsic magnetic moments. Radicals are also utilized but typically magnetic hysteresis demands the presence of higher individual magnetic moments. Nevertheless, radicals can be useful in SMMs that take advantage of exchange coupling, as they can act as intermediates that promote the alignment of spins in the metal ions. Additionally, radicals may also be used to augment the properties of the SMM. For instance, there is evidence that suggests that exchange coupling reduces the quantum tunneling of magnetization (QTM), which is one of the major components that leads to magnetic relaxation and limits the performance of SMMs.[81]

Magnetic relaxation refers to the mechanisms that govern the spin-flips that bring the system to a thermal equilibrium. In other words, magnetic relaxation is the process that causes the (electron) spins to become more disordered. There are several ways in which magnetic relaxation can occur in single-molecule magnets. The notable ones include the aforementioned QTM, thermal-assisted QTM, and the Orbach, Raman, and direct processes.[86] To understand these relaxation pathways qualitatively, one must be familiar with the electronic structures of transition metals and lanthanides, and their intricacies. The next section aims to elucidate these concepts before going back to magnetic relaxation pathways.

4.1.1 Transition Metal and Lanthanide Ions

In the development of single-molecule magnets and other magnetic species, transition metals and lanthanides are often utilized due to their large intrinsic magnetic moments. The large magnetic moments arise from unpaired spins of electrons in *d*- or *f*-type atomic orbitals, which rarely participate in covalent bonding due to their spatially contracted shapes. In addition, the *d*- and *f*-orbitals can possess large angular momentum quantum numbers, which also contribute to the magnetic moment, when all the *d*- or *f*-orbitals are not half or fully occupied. This phenomenon is often called spin-orbit coupling in literature, and it is typically much more pronounced in lanthanide-ions.

The *d*-orbitals in transition metals are degenerate in the absence of ligands. However, this degeneracy is lifted when a certain type of ligand field is introduced—for instance octahedral or tetrahedral.[11,19] This splitting of orbital energies is typically detrimental to the design of SMMs, because a large energy gap caused by a strong ligand field facilitates a low-spin state.

Therefore, implementing a weak-ligand field tends to be more beneficial to promote the high-spin state. Also, the high-spin state is thermally favored, as in high temperatures there will be more energy to excite the paired electrons over the so-called lattice-energy gap. There are also other methods for controlling the spin-state of transition metals, such as photons and pressure. These methods that do not rely on high temperatures are exciting for SMM design, as they allow for high-spin transition metal ions while keeping the temperature low to preserve magnetic hysteresis.

Contrary to the electronic structures of transition metals having a large dependence on the ligand field, the ligand field splitting of lanthanide *f*-orbitals is much weaker. Instead, the energies of different electron configurations of the *f*-orbitals are typically defined by spin-orbit coupling. In short, spin-orbit coupling explains how the total magnetic moment of a lanthanide is composed of both the spin component and the angular momentum component.[19,87] As a result, there are various possible *f*-orbital structures that lead to not just two, but often multiple magnetic states, depending on the spin-multiplicity and the total angular momentum. Lanthanide ions that have an odd number of electrons are commonly called Kramers' ions, and they have the property that their magnetic states are at least doubly-degenerate in the absence of an external magnetic field. These magnetic states are called Kramers' doublets and they are important in the pursuit of the bistable ground state for SMMs. Figure 2 illustrates the orbital diagram of transition metal *d*-orbitals in an octahedral ligand field, and an energy level diagram including relaxation pathways of the spin-orbit states in an imaginary Kramers' ion.

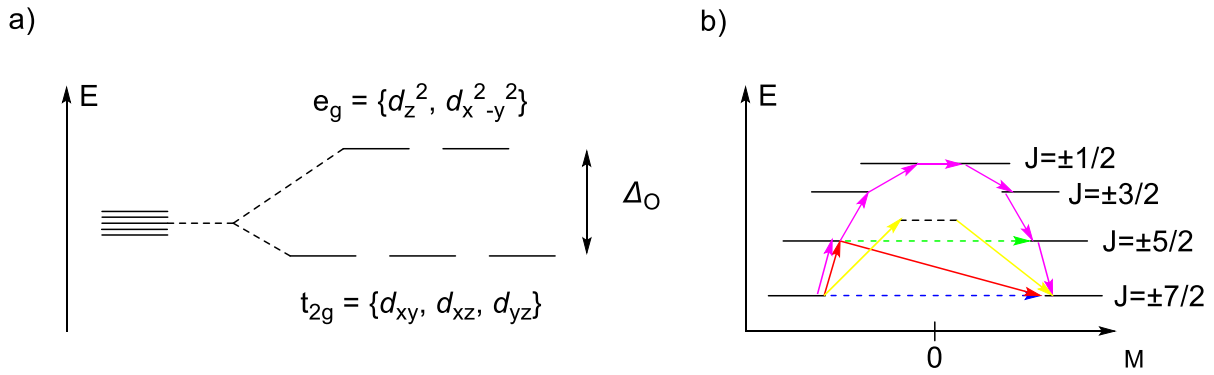

Figure 2. a) Octahedral ligand field splitting Δ_O of *d*-orbitals in transition metal complexes. b) The spin-orbit states of an imaginary Kramers' ion. J denotes the total angular momentum quantum number which is a sum of the angular momentum and spin quantum numbers, J = L + S. The arrows represent magnetic relaxation pathways: Purple = direct, red = Orbach, yellow = Raman, dashed blue = QTM, and dashed green = thermally assisted QTM.

In transition metals and lanthanides, magnetic relaxation occurs through several processes. In a magnetic ground state, the electron configuration has the maximum multiplicity and the

highest possible supporting total angular momentum. In the case of the Kramers' ion and also other bistable systems, in the absence of an external field there are two ground states, where the magnetic moments are antiparallel to each other. In transition metals in ligand fields, the electrons can be brought down to the *d*-orbitals that are lower in energy in that corresponding ligand field, causing a high-spin to low-spin transition. This transition can be facilitated, for example, by lowering the temperature. The LS to HS transition was already discussed in the previous paragraphs but in short, thermal energy, light or pressure can be used to excite the electrons from the more stable *d*-orbitals to the other *d*-orbitals, de-pairing them. Spin-orbit coupling is often dismissed in the discussion on transition metal complexes because the ligand field effects are typically dominant. This is however not the case with lanthanides, and more complex relaxation mechanisms emerge (Fig. 2b). In lanthanides, thermal energy instead excites the electrons into higher spin-orbit states, which results in a change in angular momentum quantum numbers. The excited state can then decay into one of the lower states. In the Orbach process, this decay leads to a lower magnetic state with a magnetic moment in the opposite direction. The Raman process is similar, but in it, the excitation leads to a virtual state that immediately decays and is not observable. Both Orbach and Raman processes depend on phonons causing the excitations in the first place, which can be mitigated by lowering the thermal energy and with certain coordination geometries. In addition to these direct processes, QTM and thermally assisted QTM, can cause the system to undergo a transformation without an external excitation. This effect can be mitigated by certain ligand field symmetries, large magnetic moments, and by choosing ligands that complement the anisotropy of the magnetic orbitals.[87,88]

4.1.2 Anisotropic Magnetic Moments in Single-Molecule Magnets

The anisotropy of magnetic moment is a key property in the design of lanthanide SMMs, particularly single-ion magnets (SIMs). This is because by utilizing this phenomenon, not only can the relaxation mechanisms be suppressed, but also the magnetic moment can be aligned with the shape of the molecule. This is crucial for practical applications in, for example, quantum computing and spintronics. Therefore, the design of lanthanide SMMs is often driven by anisotropy considerations.[19,89]

Anisotropic magnetic moments are a product of lanthanide, and to some extent transition metal electron structures. Only lanthanides will be considered for the sake of simplicity. The *f*-orbitals are more contracted in shape than *d*-orbitals, which explains why the ligand field splitting in them is considerably weaker than in transition metal *d*-orbitals. In addition, the angular momentum quantum numbers range from -3 to 3 in the *f*-orbitals, which creates more

flexibility in the spin-orbit states than in *d*-orbitals, and because of these two effects, spin-orbit coupling dominates the splitting of the *f*-orbital energies in many lanthanides and their ions. Another significant property that the *f*-orbitals have is their shape. The orbitals with large angular momentum quantum numbers are more oblate, while the opposite is true with the orbitals with the orbitals the angular momentum quantum number of which are closer to zero. Oblate meaning that the shape is squished on two poles and prolate meaning elongated on the poles. While this effect is also seen in *d*-orbitals, it is more prominent in *f*-orbitals. When electrons occupy these orbitals, the arising electron density is seldom spherically symmetric, but instead oblate or prolate. Consequently, the magnetic moment tends to align along the axis defining the poles. This type of magnetic moment that is connected to the electron structure is what we call an anisotropic magnetic moment.[89]

Anisotropic magnetic moments arise from the interactions of the magnetic ions with their ligand fields. It has been shown that an intuitive approach exists for improving the qualities of lanthanide SMMs by altering the *f*-orbital energies by specific arrangements of ligands[89]: With lanthanide species where the ground state corresponds to an oblate electron density, the ground state can be further stabilized from excited states by introducing a strong axial ligand field. The electrostatic repulsions between electrons in the ligand and an *f*-orbital electron is higher if the *f*-electron is on a prolate orbital. This increases the energy difference of the oblate ground state and the more prolate excited states. The opposite is true for lanthanides where the ground state density is prolate, and the ligand field is strongly equatorial. By increasing the energy gaps, thermally dependent relaxation pathways are suppressed, which is turn increases the blocking temperature. It is easy to see why this method has been so successful in designing better and better lanthanide-based SMMs.

In DFT, modelling anisotropic magnetic moments is not a well-known area of research, and several popular methods in the field have difficulties in addressing magnetic anisotropy. For instance, a simple Slater determinant is insufficient in portraying all the spin-orbit states, which is the one of the biggest limitations of DFT approaches in determining exchange coupling. Because of the severe limitations in this approach, gadolinium(III) is often chosen for DFT among the lanthanides, because its magnetic moment is isotropic due to all of its *f*-orbitals being singly occupied.[9]

4.2 Computational Investigations in Molecular Magnetism

Computational and experimental methods are often used in tandem when probing the magnetic properties of molecular magnets. This section is devoted to reviewing instances of computational analysis, particularly DFT, on the magnetic properties of molecular magnets.

The discussion focuses heavily on exchange coupling and related effect, and it aims to highlight the ways in which DFT was used to support experimental data and to help explain the magnetic properties of molecules and molecular materials.

4.2.1 Molecular Dithiadiazolyl Radical-Based Materials

Organic radical-based molecular materials have been a significant topic of interest since the early years of molecular magnetism. Among these radical-based materials, a family of stable sulfur-nitrogen radicals, dithiadiazolyls (Fig. 3a), have been thoroughly researched over the years, as they at one point seemed promising candidates for organic ferromagnets.[90] Some of these species were observed to exhibit magnetic ordering at temperatures as high as 36 K.[91]

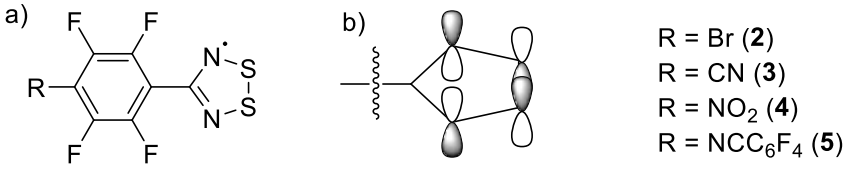

Figure 3. a) Molecular structures of the dithiadiazolyl radical-based materials (**2**–**5**) investigated by Rawson *et al*..[10] b) The magnetic π*-orbital in the dithiadiazolyl heterocycle in which the unpaired electron is delocalized.

These dithiadiazolyl radicals (**2**-**5**) have been analyzed with DFT by Rawson *et al* in 2005.[10] The authors employed the B3LYP global hybrid functional with the GTO-type TZ basis set 6-311G**.[92] A DZ basis set, 6-31G**[92] was also tested with no significant discrepancies in the results. They calculated the exchange coupling constants by using the Yamaguchi projection (Eq. 63).

Their analysis suggested that the intermolecular coupling between the molecules in each material included both antiferromagnetic and ferromagnetic couplings, with coupling constants of up to ±60 cm^{-1}. The results also allude to the main mechanism of coupling being the direct exchange between the dithiadiazolyl magnetic orbitals (Fig. 3b). Strong exchange couplings in these molecules are limited to proximate heterocycles, in which ferromagnetic coupling arises from accidental orthogonality of the magnetic, heterocyclic π*-orbitals. In (**4**) and (**5**), the structure is defined by interactions between the side group and the sulfurs of the dithiadiazolyl molecule, while dipolar interactions between the sulfur and nitrogen atoms, or dispersion between two sulfur atoms also contributes to the structure. Alternatively, the structure can be mostly defined by the latter interactions, leading to slipped π-stacked systems with alternating layers, as in materials of molecules (**2**) and (**3**). With these systems, some of the strongest couplings were calculated. The couplings between two molecules in a stack could also alternate between antiferromagnetic and ferromagnetic, depending on if the π*-orbitals overlap. On molecule (**2**) the crystal structure enabled two axes of strong exchange coupling according to

computational results. On one of the axes, the coupling alternates between antiferromagnetic and ferromagnetic, while on the other axis the coupling is purely antiferromagnetic. However, no long-range ordering is observed, which could be explained with the low anisotropy of the magnetic orbitals combined with different exchange coupling types with similar strength. This illustrates the difficulty in designing organic ferromagnets, as very specific molecules are required to extend the coupling to more than one axis, and at the same time systematic couplings are needed to produce long-range ferromagnetic ordering.

4.2.2 Vanadyl(II)–Copper(II) Clusters

Between 1978 and 1981, Kahn and coworkers[69,70] introduced the concept of an orbital symmetry approach to the design of exchange-coupled systems by investigating a complex (**6**) containing one VO^{2+} ion and one Cu^{2+} ion (Fig. 4a). The authors argued that the ferromagnetic coupling seen in the complex arises from the orthogonality of the two magnetic orbitals. This was evidenced by magnetic susceptibility measurements, from which a value of 59 cm^{-1} was calculated for the exchange coupling constant.[v] Based on the susceptibility data, it was also concluded that intermolecular coupling is negligible.

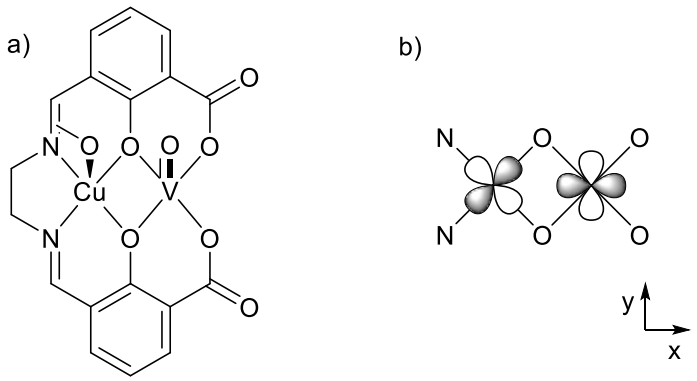

Figure 4. a) The Lewis-structure of the cluster (**6**) reported by Kahn *et al.*.[69] The oxo- and methyl groups that coordinate to Cu(II) and V(II), respectively, protrude from the xy-plane. b) The magnetic orbitals in substance 6. The d_{xy}-orbital belonging to Cu(II) is on the left, while the $d_{x^2-y^2}$-orbital in V(II) is on the right.

The theoretical and experimental studies were later supported by quantum chemistry calculations. Broken symmetry DFT calculations by Costa *et al.*[93] predicted exchange-coupling constants (J) of around 50 cm^{-1} which were in line with the experimental value of 59 cm^{-1}. The coupling constants obtained from BS-DFT calculations on average surpassed those from wave-function based methods in accuracy relative to the experimental value. The closest matching J

[v] Original experimental and computational data on exchange coupling was gathered by the authors by using J in equations instead of $2J$, and the original values have been altered here to match equations (59) and (61–65). Similar adjustments have been done for the data on compounds (**2-5**) and (**10-13**).

value, 58 cm^{-1}, was given by the M06 global hybrid functional[39,40] with the 6-31G(d) all-electron GTO basis set. The M06 functional is composed of meta-GGA functionals and 27% exact exchange. Between other combinations of functionals and basis sets tested, the *J* values ranged from 36 to 63. The wave-function methods tested predicted values from 20 to 41, significantly lower than the DFT and experimental values. The authors also used these computational methods to predict exchange coupling in other known systems, with very different results. Among the 6 compounds tested by them, LC-ωPBE[50–52] performed the best in predicting the coupling constants. These findings support the idea that exchange-correlation functionals are very sensitive to the system under investigation and the quantities that are being calculated.

While the experimental and computation data does not directly show a correlation between the orthogonality of the magnetic orbitals and the ferromagnetic coupling between them, this can be hypothesized based on the electron structures of the vanadium and copper atoms, and the ligand field. In this molecule, Cu(II) has the electron structure $[Ar]3d^9$ and V(II) has the structure $[Ar]3d^14s^2$. This means that both atoms have one unpaired electron, each on a *d*-orbital. The ligand field then splits the energies of these orbitals, so that the energetically highest Cu(II) *d*-orbital, d_{xy}, directly faces all the ligands and the energetically lowest, $d_{x^2-y^2}$ *d*-orbital in V(II) does not overlap with any ligands (Fig 4b). Thus, the energetically highest *d*-orbital in Cu(II) is only half-full, while the energetically lowest *d*-orbital in V(II) is the only one containing an electron, and therefore these orbitals are the magnetic orbitals and are strictly orthogonal due to the ligand field.

4.2.3 Radical-Bridged Lanthanide Dimers

In 2011, Long *et al.*[81] reported a family of radical-bridged lanthanide dimers (Fig. 5), among which the dysprosium complex (**7**) exhibited promising single-molecule magnet behavior. These types of three-center magnetic molecules were used as an example in section 3.2 when demonstrating the use of the HDvV Hamiltonian. It can be argued that in these types of molecules, the exchange coupling may facilitate magnetic relaxation if the coupling is weak. This drop in performance is sometimes elevated by a reduction in anisotropy arising from an increased number of magnetic centers. If these effects could be minimized and simultaneously the size of the system increased and the exchange coupling strengthened, a new generation of high-performance single-molecule magnets might emerge.

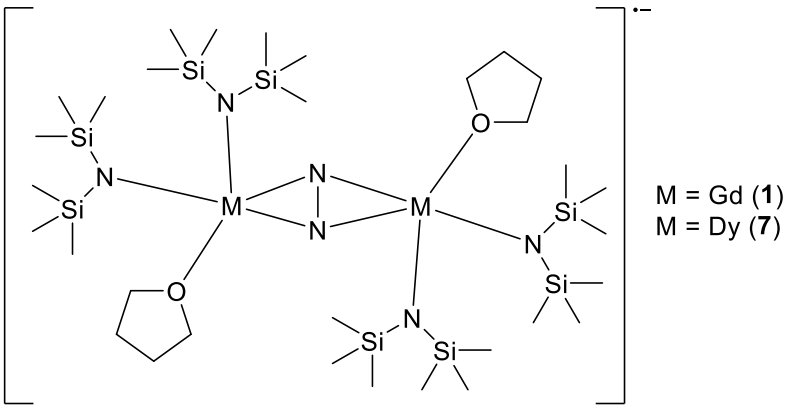

Figure 5. The radical-bridged lanthanide dimers (**1** and **7**) first reported by Long *et al.*.[81] The Gd analogue expressed the highest exchange-coupling constant, while the Dy counterpart is a single-molecule magnet.

The molecules synthesized by Long *et al.*[81] have the structure shown in figure 5. The gadolinium complex (**1**) holds a measured gadolinium–radical exchange-coupling constant of -27 cm^{-1}, a gadolinium-gadolinium coupling constant of -0.49 cm^{-1}, and an intermolecular exchange-coupling constant of 0.07 cm^{-1} as evidenced by magnetic susceptibility data. The dysprosium counterpart was found to have a blocking temperature of 8.3 K. These findings support the idea that integrating strong exchange coupling, whether ferromagnetic or antiferromagnetic, may lead to a prominent strategy for designing SMMs with higher blocking temperatures.

(**1**) also led researchers to accumulate a wealth of computational data and theoretical analysis on it. In 2012, Rajaraman and Rajeshkumar[79] explored the exchange coupling and its origins by utilizing DFT and theoretical models. They obtained *J* values of -23.7 cm^{-1} for the gadolinium-radical coupling, and -0.53 cm^{-1} for Gd-Gd coupling, which are in good agreement with experimental data. The values were calculated using a broken symmetry approach[94] on the DFT energies. They used the B3LYP global hybrid functional with the CS[59] basis set for Gd and the TZV[95,96] basis set for all other atoms. The results showed that the pseudopotential proposed by Cundari and Stevens for gadolinium can work exceptionally well in computing exchange coupling constants in coupled gadolinium systems. In an article published two years later, Rajaraman *et al.*[97] examined a variety of DFT methods for calculating the coupling constants on a variety of molecules, including the one discussed here. Surprisingly, they found that not only is the CS pseudopotential viable, but it seems to give more accurate values for the coupling constants in this molecule compared to other methods, which may result from relativistic effects being included in the pseudopotential.

Based on theoretical models combined with the DFT data, Rajaraman and coworkers[97] reasoned that the empty 5*d*-, 6*s*-, and 6*p*-orbitals participate in the mechanism leading to magnetic coupling between the moieties, in addition to the half-filled 4*f*-orbitals. It was also

discovered that 5*d*-orbitals are involved in this so-called Goodenough's mechanism[98] by computational study of Vieru *et al.*.[99] Recall from chapter 3 that exchange coupling has two components: the overlap integral promoting antiferromagnetic coupling and the exchange integral which contributes to ferromagnetic coupling. Due to the contracted nature of the *f*-orbitals, these integrals tend to have small values, which corresponds to weak exchange coupling. However, the diffuse shape of the magnetic π*-orbital in the N_2^{3-} radical causes it to sufficiently extend to the lanthanide 4*f*-orbitals, yielding relatively strong coupling as a result. Additionally, the charge difference between the radical and gadolinium facilitates a charge transfer mechanism that partially populates the unoccupied 5*d*-, 6*s*-, and 6*p*-orbitals, removing the same fraction of population from the magnetic orbital in the radical. Due to the orthogonality between atomic orbitals of the same atom, the charge transfer mechanism adds a ferromagnetic contribution, although it is not strong enough to overcome the antiferromagnetic contribution from the 4*f*-π* overlap, as evidenced by the negative exchange coupling constants.

As another example of radical-bridged lanthanide dimers, Murugesu *et al.*[80] reported a Dy^{3+} dimer with two bridging radical ligands (**8**, Fig. 6) in addition to its Y^{3+} counterpart (**9**). These molecules were among the first to include coordination-induced intramolecular π-π interactions—also known as a multi-centered π-π bond or pancake bond—between radical ligands, which has the benefit of suppressing direct radical dimerization. This multi-centered π-π bond results in a strong antiferromagnetic coupling between the radicals, as evidenced by electron paramagnetic resonance (EPR) spectroscopy studies on the yttrium dimer (**9**). Additionally, the dysprosium dimer (**8**) shows SMM behavior below 8 K based on magnetic susceptibility measurements, and the magnetic relaxation was found to occur mostly through the QTM and Raman pathways, as the anisotropy and symmetry of the coordination environments are relatively weak. One obvious advantage these types of molecules have over the famous N_2^{3-} radical-bridged lanthanide dimers is the higher stability of the radicals due to electron delocalization.

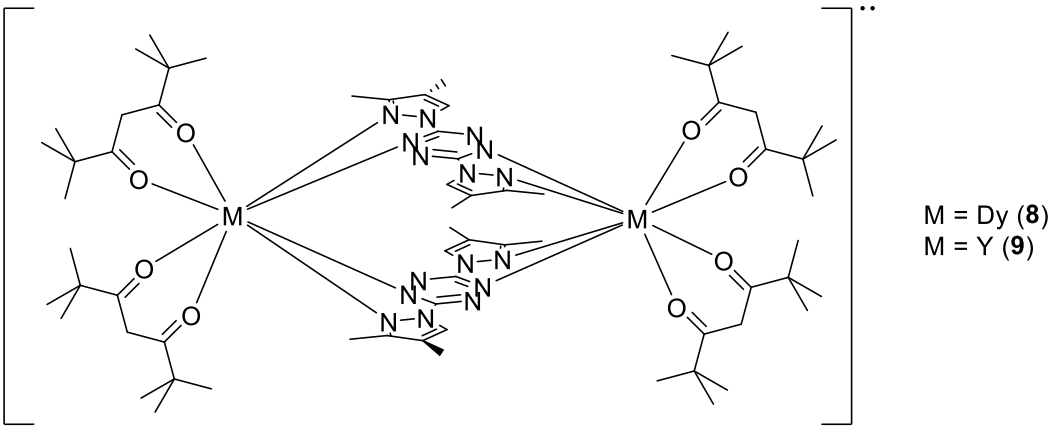

Figure 6. The structure of the Dy^{3+} dimer (**8**) and its Y^{3+} analogue (**9**) reported by Murugesu *et al.*.[80] The multi-centered π-π bond lies between the tetrazine rings of the bridging ligands.

In addition to EPR measurements, the authors analyzed the magnetic properties of the yttrium dimer (**9**) with BS-DFT and multiconfigurational wave function-based methods in the same article.[80,vi] Among the tested functionals and basis sets, the adiabatic and non-adiabatic singlet-triplet gaps directly corresponding to the exchange-coupling constant between the radicals, evaluated with the Yamaguchi projection, were calculated to be in the order of several thousand wavenumbers, suggesting a large degree of covalency. Based on geometry optimization and experimental crystal data, the best performing methods included B3LYP-D3/def2-TZVP, PBE0-d3/def2-TZVP and LC-ωPBE-D3/def2-TZVP. The multiconfigurational wave function-based calculations were used to shed light on the nature of the multi-centered π-π bond. It was discovered that the bonding is roughly half covalent, meaning that the other half represents a diradical state. This gives a significant reason to be skeptical towards the broken symmetry calculations, as in this scenario the state of the molecule is far from what is representable with a single Slater determinant. Nevertheless, the large covalent character of the multi-centered π-π bond is strong evidence towards the exceptional antiferromagnetic coupling predicted with DFT.

The multi-centered π-π bonding and antiferromagnetic coupling in (**8**) and (**9**) can also be rationalized from the perspective of orbital symmetry and orthogonality. Because the bridging radical ligands are identical and the molecule is centrosymmetric, it is reasonable to assume that the SOMOs are also identical. Therefore, they can only be accidentally orthogonal, which is unlikely considering that the peaks of one SOMO would have to align with the nodes of the other extremely precisely for the overlap integral and the resulting bonding to vanish. Had accidental orthogonality occurred, the experiments would have suggested a triplet ground state for (**9**), and the multi-centered π-π bond would have near-zero covalent character. Compared to (**1**), the blocking temperature of (**8**) is very similar, but the exchange-coupling between these types of bridged dimers varies significantly. Because of the large antiferromagnetic coupling and the related covalent character of the multi-centered π-π bond in (**8**), the dysprosium-radical coupling is negligible. Thus, it can be argued that the performance of (**8**) as a SMM is purely based on the ligand field around each Dy^{3+} ion, since the Dy-Dy coupling in (**8**) is only 0.016 cm^{-1} as measured by Murugesu *et al.*.[80] With ferromagnetic intramolecular exchange coupling it may be possible to enhance the magnetic properties of lanthanide dimers, because the

[vi] Multiconfigurational refers to using multiple configuration state functions. Multiconfigurational methods are also known as complete active space self-consistent field (CASSCF) calculations.

coupling would introduce a new level of magnetic states and increase the thermal magnetic reversal barrier this way. These ferromagnetically coupled bridging radical ligands could also open a way for increasing the spin-orbit splitting and implementing a certain ligand field to suppress all forms of magnetic relaxation, although doing this in practice seems extraordinarily difficult.

As yet another example of radical-bridged lanthanide dimers, Long *et al.*[100] have investigated the effects of chemical substitution of the bridging radical on the magnetic properties in a family of 2,2'-bipyrimidine bridged lanthanide dimers. Out of the tested molecules, the gadolinium dimers (Fig. 7) were examined with BS-DFT, and their dysprosium analogues show SMM behavior. The authors found a strong connection between the chemical substitution and strength of exchange coupling between a gadolinium and the bridging radical, while their dysprosium counterparts show varying total spin-orbit splitting—in other words, the relaxation barrier—and, thus, different magnetic relaxation behavior. The results presented by the authors show that side groups that withdraw electron density enhance both the exchange coupling and spin-orbit splitting, suggesting a simple strategy for improving the performance of single molecule magnets.

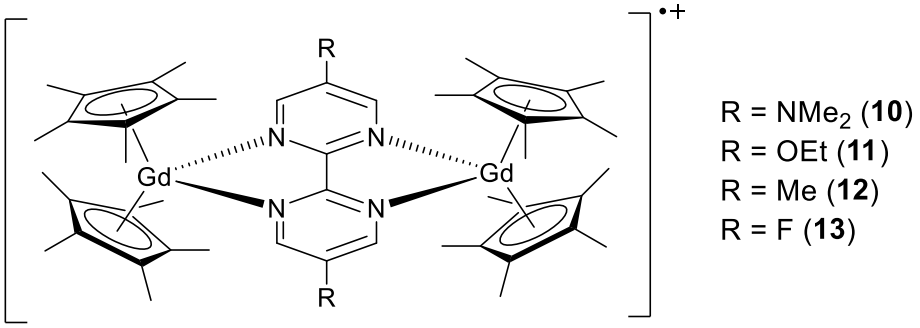

Figure 7. The structures of the gadolinium dimers (**10**–**13**) studied by Long *et al.*.[100]

In their DFT study, Long *et al.*[100] used the crystal structures of the corresponding dysprosium dimers and replaced the Dy^{3+} ions with Gd^{3+} ions for the calculation in order to estimate the exchange coupling in the dysprosium variants. The exchange coupling constants obtained with B3LYP/SVP did not show the drastic substitution dependence experimentally determined from the gadolinium dimers. Whether this results from the different geometry or from the possible inaccuracy of DFT is unclear, but the values of the coupling constants fell into a similar range (~ -5 cm^{-1}). Therefore, it can be argued that there is more evidence towards the geometry playing a significant role in the substitution dependence of the exchange coupling and spin-orbit splitting, instead of the failure resulting from DFT. The alternative explanation is plausible too, as exchange coupling constants are known to heavily depend on the functional and basis

set used. Maybe the basis set was too limited to correctly model the orbitals in a way in which the substitution dependence would surface.

The data gathered by Long *et al.*[100] is quite interesting as it introduces a somewhat new strategy for improving SMMs that utilize exchange coupling, and it provides clues on the functionality of DFT in exchange coupled systems. Further research into the effects of XC functional and basis set on this subject could produce intriguing results on what size and functions a basis set must have to accurately predict the effect of chemical substitution on exchange coupling. As a sidenote, the authors also ran multiconfigurational calculations to determine the strength of the spin-orbit splitting, and found a similar dependence on chemical substitution, which indicates that multiconfigurational methods can describe the phenomenon.

5 Conclusion

Density functional theory has attracted considerable attention since its birth in the mid-1960s, and it has become a quintessential computational method. This is especially true in chemistry due to its lesser computational cost compared to many wave function-based alternatives, which also makes DFT a good choice for larger systems. Lately, DFT has been used in conjunction with broken symmetry approaches to predict exchange coupling between magnetic centers in molecules and materials. Research has shown that these methods can indeed replicate experimentally determined coupling constants with a high degree of accuracy. However, one should be careful when employing these methods as the calculated coupling tends to depend heavily on the exchange-correlation functional and basis set used. In addition, because the system is represented by a single determinant in KS-DFT, it is difficult to capture spin-orbit splitting and other intricate effects that contribute to magnetism and exchange coupling. This somewhat limits the application of DFT to molecules that have isotropic magnetic moments, but for example with lanthanide-based coupled systems it is possible to use isotropic alternatives, such as Gd^{3+} instead of other lanthanide ions, for calculating exchange coupling constants.

Currently, there is a substantial amount of exchange coupling data from DFT calculations of known molecules. In principle, DFT could be used to predict magnetic coupling in novel, hypothetical molecules. However, the strong functional- and basis set dependence of exchange coupling in different systems somewhat hinders this approach. Therefore, if DFT is used in this manner, thorough validation of functionals and basis sets on similar, known molecules is mandatory. With the development of new functionals and DFT basis sets, this burden might be lessened in the future, but the limitations of the Slater determinant will always persist in KS-DFT.

The field of molecular magnetism is still quite active, although its popularity has slowly stagnated from the decline of attention towards organic ferromagnets which once represented a major part of the field. With no apparent way to make progress towards organic ferromagnets, focus shifted to transition metal clusters and later to lanthanide complexes, too. Some of these species exhibit single-molecule magnet behavior in that they retain magnetization in zero field for extended periods of time. These so-called single-molecule magnets comprise a large portion of research in the field today, with prospects of using them in quantum computing, high-density information storage devices, and spintronics. Exchange coupling could provide a path for the design of novel single-molecule magnets with enhanced properties, although for now the position of the best-performing single-molecule magnet is held by a lanthanide complex with an extremely axial ligand field which maximizes the magnetic anisotropy of the lanthanide ion.[85]

References

1. Hohenberg, P. and Kohn, W., Inhomogeneous electron gas, *Phys. Rev.*, **1964**, *136*, B864.
2. Kohn, W. and Sham, L. J., Self-consistent equations including exchange and correlation effects, *Phys. Rev.*, **1965**, *140*, A1133.
3. Koch, W. and Holthausen, M. C., *A Chemist's Guide to Density Functional Theory*, Wiley, 2001.
4. Jones, R. O., Density functional theory: Its origins, rise to prominence, and future, *Rev. Mod. Phys.*, **2015**, *87*, 897.
5. Slater, J. C., Note on hartree's method [5], *Phys. Rev.*, **1930**, 35, 210–211.
6. Fock, V., Näherungsmethode zur Lösung des quantenmechanischen Mehrkörperproblems, *Zeitschrift für Phys.*, **1930**, *61*, 126–148.
7. Thomas, L. H., The calculation of atomic fields, *Math. Proc. Cambridge Philos. Soc.*, **1927**, *23*, 542–548.
8. Fermi, E., Un Metodo Statistico per la Determinazione di alcune Prioprietà dell'Atomo, *Rend. Accad. Naz. Lincei*, **1927**, *6*, 602–607.
9. Gupta, T.; Rajeshkumar, T. and Rajaraman, G., Magnetic exchange in {GdIII-radical} complexes: Method assessment, mechanism of coupling and magneto-structural correlations, *Phys. Chem. Chem. Phys.*, Royal Society of Chemistry, 2014, pp. 14568–14577.
10. Rawson, J. M.; Luzon, J. and Palacio, F., Magnetic exchange interactions in perfluorophenyl dithiadiazolyl radicals, *Coord. Chem. Rev.*, **2005**, 249, 2631–2641.
11. Atkins, P.; de Paula, J. and Keeler, J., *Atkins' Physical Chemistry*, 11th edition, Oxford

University Press, 2018.

12. Anderson, P. W., New approach to the theory of superexchange interactions, *Phys. Rev.*, **1959**, *115*, 2–13.
13. Heisenberg, W., Zur Theorie des Ferromagnetismus, *Zeitschrift für Phys.*, **1928**, *49*, 619–636.
14. Noodleman, L.; Norman, J. G.; Osborne, J. H.; Aizman, A. and Case, D. A., Models for Ferredoxins: Electronic Structures of Iron-Sulfur Clusters with One, Two, and Four Iron Atoms, *J. Am. Chem. Soc.*, **1985**, *107*, 3418–3426.
15. Noodleman, L. and Davidson, E. R., Ligand spin polarization and antiferromagnetic coupling in transition metal dimers, *Chem. Phys.*, **1986**, *109*, 131–143.
16. Noodleman, L., Valence bond description of antiferromagnetic coupling in transition metal dimers, *J. Chem. Phys.*, **1981**, *74*, 5737–5743.
17. Dirac, P. A. M., On the theory of quantum mechanics, *Proc. R. Soc. London. Ser. A, Contain. Pap. a Math. Phys. Character*, **1926**, *112*, 661–677.
18. van Vleck, J. H., *Electric and Magnetic Susceptibilities*, Clarendon Press: Oxford, 1932.
19. Gatteschi, D.; Bogani, L.; Cornia, A.; Mannini, M.; Sorace, L. and Sessoli, R., Molecular magnetism, status and perspectives, *Solid State Sci.*, **2008**, *10*, 1701–1709.
20. Born, M. and Oppenheimer, R., Zur Quantentheorie der Molekeln, *Ann. Phys.*, **1927**, *389*, 457–484.
21. Hartree, D. R., The Wave Mechanics of an Atom with a Non-Coulomb Central Field Part I Theory and Methods, *Math. Proc. Cambridge Philos. Soc.*, **1928**, *24*, 89–110.
22. Koopmans, T., Über die Zuordnung von Wellenfunktionen und Eigenwerten zu den Einzelnen Elektronen Eines Atoms, *Physica*, **1934**, *1*, 104–113.
23. Löwdin, P. O., Scaling problem, virial theorem, and connected relations in quantum mechanics, *J. Mol. Spectrosc.*, **1959**, *3*, 46–66.
24. Pople, J. A. and Nesbet, R. K., Self-consistent orbitals for radicals [13], *J. Chem. Phys.*, **1954**, 22, 571–572.
25. Roothaan, C. C. J., Self-Consistent field theory for open shells of electronic systems, *Rev. Mod. Phys.*, **1960**, *32*, 179–185.
26. Griffiths, D. J. and Schroeter, D. F., *Introduction to quantum mechanics*, 3rd edition, Cambridge University Press, Cambridge, 2018.
27. Wigner, E. and Seitz, F., On the constitution of metallic sodium, *Phys. Rev.*, **1933**, *43*, 804–810.
28. Slater, J. C., A simplification of the Hartree-Fock method, *Phys. Rev.*, **1951**, *81*, 385–390.

29. Gáspár, R., Über eine Approximation des Hartree-Fockschen Potentials Durch eine Universelle Potentialfunktion, *Acta Phys. Acad. Sci. Hungaricae*, **1954**, *3*, 263–286.
30. Gunnarsson, O. and Lundqvist, B. I., Exchange and correlation in atoms, molecules, and solids by the spin-density-functional formalism, *Phys. Rev. B*, **1976**, *13*, 4274–4298.
31. Levy, M., Universal variational functionals of electron densities, first-order density matrices, and natural spin-orbitals and solution of the v-representability problem, *Proc. Natl. Acad. Sci. U. S. A.*, **1979**, *76*, 6062–6065.
32. Lieb, E. H., Density functionals for coulomb systems, *Int. J. Quantum Chem.*, **1983**, *24*, 243–277.
33. Dirac, P. A. M., The quantum theory of the electron, *Proc. R. Soc. London. Ser. A, Contain. Pap. a Math. Phys. Character*, **1928**, *117*, 610–624.
34. Parr, R. G. and Yang, W., *Density-Functional Theory of Atoms and Molecules*, Oxford University Press, 1989.
35. Harris, J., Adiabatic-connection approach to Kohn-Sham theory, *Phys. Rev. A*, **1984**, *29*, 1648–1659.
36. Perdew, J. P.; Burke, K. and Ernzerhof, M., Generalized gradient approximation made simple, *Phys. Rev. Lett.*, **1996**, *77*, 3865–3868.
37. Wang, Y. and Perdew, J. P., Correlation hole of the spin-polarized electron gas, with exact small-wave-vector and high-density scaling, *Phys. Rev. B*, **1991**, *44*, 13298–13307.
38. Curtiss, L. A.; Raghavachari, K.; Redfern, P. C. and Pople, J. A., Assessment of Gaussian-2 and density functional theories for the computation of enthalpies of formation, *J. Chem. Phys.*, **1997**, *106*, 1063–1079.
39. Zhao, Y. and Truhlar, D. G., A new local density functional for main-group thermochemistry, transition metal bonding, thermochemical kinetics, and noncovalent interactions, *J. Chem. Phys.*, **2006**, *125*, 194101.
40. Zhao, Y. and Truhlar, D. G., The M06 suite of density functionals for main group thermochemistry, thermochemical kinetics, noncovalent interactions, excited states, and transition elements: Two new functionals and systematic testing of four M06-class functionals and 12 other functionals, *Theor. Chem. Acc.*, **2008**, *120*, 215–241.
41. Becke, A. D., Density-functional thermochemistry. III. The role of exact exchange, *J. Chem. Phys.*, **1993**, *98*, 5648–5652.
42. Becke, A. D., Density-functional thermochemistry. III. The role of exact exchange, *J. Chem. Phys.*, **1993**, *98*, 5648–5652.
43. Adamo, C. and Barone, V., Toward reliable density functional methods without adjustable parameters: The PBE0 model, *J. Chem. Phys.*, **1999**, *110*, 6158–6170.

44. Becke, A. D., Density-functional exchange-energy approximation with correct asymptotic behavior, *Phys. Rev. A*, **1988**, *38*, 3098–3100.
45. Lee, C.; Yang, W. and Parr, R. G., Development of the Colle-Salvetti correlation-energy formula into a functional of the electron density, *Phys. Rev. B*, **1988**, *37*, 785–789.
46. Stephens, P. J.; Devlin, F. J.; Chabalowski, C. F. and Frisch, M. J., Ab Initio calculation of vibrational absorption and circular dichroism spectra using density functional force fields, *J. Phys. Chem.*, **1994**, *98*, 11623–11627.
47. Ernzerhof, M. and Scuseria, G. E., Assessment of the Perdew-Burke-Ernzerhof exchange-correlation functional, *J. Chem. Phys.*, **1999**, *110*, 5029–5036.
48. Perdew, J. P.; Burke, K. and Ernzerhof, M., Erratum: Generalized gradient approximation made simple (Physical Review Letters (1996) 77 (3865)), *Phys. Rev. Lett.*, **1997**, 78, 1396.
49. Toulouse, J.; Colonna, F. and Savin, A., Long-range - Short-range separation of the electron-electron interaction in density-functional theory, *Phys. Rev. A - At. Mol. Opt. Phys.*, **2004**, *70*, 062505.
50. Vydrov, O. A. and Scuseria, G. E., Assessment of a long-range corrected hybrid functional, *J. Chem. Phys.*, **2006**, *125*, 234109.
51. Krukau, A. V.; Vydrov, O. A.; Izmaylov, A. F. and Scuseria, G. E., Influence of the exchange screening parameter on the performance of screened hybrid functionals, *J. Chem. Phys.*, **2006**, *125*, 224106.
52. Vydrov, O. A.; Scuseria, G. E. and Perdew, J. P., Tests of functionals for systems with fractional electron number, *J. Chem. Phys.*, **2007**, *126*, 154109.
53. Yanai, T.; Tew, D. P. and Handy, N. C., A new hybrid exchange-correlation functional using the Coulomb-attenuating method (CAM-B3LYP), *Chem. Phys. Lett.*, **2004**, *393*, 51–57.
54. Roothaan, C. C. J., New developments in molecular orbital theory, *Rev. Mod. Phys.*, **1951**, *23*, 69–89.
55. Hehre, W. J.; Stewart, R. F. and Pople, J. A., Self-consistent molecular-orbital methods. I. Use of gaussian expansions of slater-type atomic orbitals, *J. Chem. Phys.*, **1969**, *51*, 2657–2664.
56. Weigend, F. and Ahlrichs, R., Balanced basis sets of split valence, triple zeta valence and quadruple zeta valence quality for H to Rn: Design and assessment of accuracy, *Phys. Chem. Chem. Phys.*, **2005**, *7*, 3297–3305.
57. Balasubramani, S. G.; Chen, G. P.; Coriani, S.; Diedenhofen, M.; Frank, M. S.; Franzke, Y. J.; Furche, F.; Grotjahn, R.; Harding, M. E.; Hättig, C.; Hellweg, A.; Helmich-Paris,

B.; Holzer, C.; Huniar, U.; Kaupp, M.; Marefat Khah, A.; Karbalaei Khani, S.; Müller, T.; Mack, F.; Nguyen, B. D.; Parker, S. M.; Perlt, E.; Rappoport, D.; Reiter, K.; Roy, S.; Rückert, M.; Schmitz, G.; Sierka, M.; Tapavicza, E.; Tew, D. P.; Van Wüllen, C.; Voora, V. K.; Weigend, F.; Wodyński, A. and Yu, J. M., TURBOMOLE: Modular program suite for ab initio quantum-chemical and condensed-matter simulations, *J. Chem. Phys.*, **2020**, *152*.

58. Stevens, W. J.; Krauss, M.; Basch, H. and Jasien, P. G., Relativistic compact effective potentials and efficient, shared-exponent basis sets for the third-, fourth-, and fifth-row atoms, *Can. J. Chem.*, **1992**, *70*, 612–630.
59. Cundari, T. R. and Stevens, W. J., Effective core potential methods for the lanthanides, *J. Chem. Phys.*, **1993**, *98*, 5555–5565.
60. Dolg, M.; Stoll, H. and Preuss, H., Energy-adjusted ab initio pseudopotentials for the rare earth elements, *J. Chem. Phys.*, **1989**, *90*, 1730–1734.
61. Andrae, D.; Häußermann, U.; Dolg, M.; Stoll, H. and Preuß, H., Energy-adjusted ab initio pseudopotentials for the second and third row transition elements, *Theor. Chim. Acta*, **1990**, *77*, 123–141.
62. Autschbach, J., Perspective: Relativistic effects, *J. Chem. Phys.*, **2012**, *136*, 150902.
63. Reiher, M., Douglas-Kroll-Hess theory: A relativistic electrons-only theory for chemistry, *Theor. Chem. Acc.*, **2006**, *116*, 241–252.
64. Van Lenthe, E.; Snijders, J. G. and Baerends, E. J., The zero-order regular approximation for relativistic effects: The effect of spin-orbit coupling in closed shell molecules, *J. Chem. Phys.*, **1996**, *105*, 6505–6516.
65. Muller, P., Glossary of terms used in physical organic chemistry: (IUPAC Recommendations 1994), *Pure Appl. Chem.*, **1994**, *66*, 1077–1184.
66. Grimme, S.; Antony, J.; Ehrlich, S. and Krieg, H., A consistent and accurate ab initio parametrization of density functional dispersion correction (DFT-D) for the 94 elements H-Pu, *J. Chem. Phys.*, **2010**, *132*, 241722.
67. Grimme, S.; Ehrlich, S. and Goerigk, L., Effect of the damping function in dispersion corrected density functional theory, *J. Comput. Chem.*, **2011**, *32*, 1456–1465.
68. Mansikkamäki, A. and Tuononen, H. M., The Role of Orbital Symmetries in Enforcing Ferromagnetic Ground State in Mixed Radical Dimers, *J. Phys. Chem. Lett.*, **2018**, *9*, 3624–3630.
69. Kahn, O.; Journaux, Y.; Morgenstern-Badarau, I.; Galy, J. and Jaud, J., Synthesis, Crystal Structure and Molecular Conformations, and Magnetic Properties of a CuII-VOII Heterobinuclear Complex: Interaction between Orthogonal Magnetic Orbitals, *J. Am.*

Chem. Soc., **1982**, *104*, 2165–2176.

70. Kahn, O.; Tola, P.; Galy, J. and Coudanne, H., Interaction between Orthogonal Magnetic Orbitals in a Copper(II)-Oxovanadium(II) Heterobinuclear Complex, *J. Am. Chem. Soc.*, **1978**, 100, 3931–3933.
71. Slater, J. C., Note on orthogonal atomic orbitals, *J. Chem. Phys.*, **1951**, *19*, 220–223.
72. Hicks, R. G., *Stable Radicals: Fundamentals and Applied Aspects of Odd-Electron Compounds*, John Wiley and Sons, 2010.
73. Mansikkamäki, A. and Tuononen, H. M., The Role of Orbital Symmetries in Enforcing Ferromagnetic Ground State in Mixed Radical Dimers, *J. Phys. Chem. Lett.*, **2018**, *9*, 3624–3630.
74. Kollmar, C. and Kahn, O., Ferromagnetic Spin Alignment in Molecular Systems: An Orbital Approach, *Acc. Chem. Res.*, **1993**, *26*, 259–265.
75. Yamaguchi, K.; Tsunekawa, T.; Toyoda, Y. and Fueno, T., Ab initio molecular orbital calculations of effective exchange integrals between transition metal ions, *Chem. Phys. Lett.*, **1988**, *143*, 371–376.
76. Yamaguchi, K.; Fukui, H. and Fueno, T., MOLECULAR ORBITAL (MO) THEORY FOR MAGNETICALLY INTERACTING ORGANIC COMPOUNDS. AB-INITIO MO CALCULATIONS OF THE EFFECTIVE EXCHANGE INTEGRALS FOR CYCLOPHANE-TYPE CARBENE DIMERS, *Chem. Lett.*, **1986**, *15*, 625–628.
77. Yamaguchi, K.; Jensen, F.; Dorigo, A. and Houk, K. N., A spin correction procedure for unrestricted Hartree-Fock and Møller-Plesset wavefunctions for singlet diradicals and polyradicals, *Chem. Phys. Lett.*, **1988**, *149*, 537–542.
78. Reta Mañeru, D.; Pal, A. K.; Moreira, I. D. P. R.; Datta, S. N. and Illas, F., The triplet-singlet gap in the m -Xylylene radical: A not so simple One, *J. Chem. Theory Comput.*, **2014**, *10*, 335–345.
79. Rajeshkumar, T. and Rajaraman, G., Is a radical bridge a route to strong exchange interactions in lanthanide complexes? A computational examination, *Chem. Commun.*, **2012**, *48*, 7856–7858.
80. Lemes, M. A.; Mavragani, N.; Richardson, P.; Zhang, Y.; Gabidullin, B.; Brusso, J. L.; Moilanen, J. O. and Murugesu, M., Unprecedented intramolecular pancake bonding in a {Dy2} single-molecule magnet, *Inorg. Chem. Front.*, **2020**, *7*, 2592–2601.
81. Rinehart, J. D.; Fang, M.; Evans, W. J. and Long, J. R., Strong exchange and magnetic blocking in N_2<super>3−</super>-radical-bridged lanthanide complexes, *Nat. Chem.* |, **2011**, *3*.
82. Sessoli, R.; Gatteschi, D.; Caneschi, A. and Novak, M. A., Magnetic bistability in a

metal-ion cluster, *Nature*, **1993**, *365*, 141–143.

83. Fataftah, M. S.; Zadrozny, J. M.; Rogers, D. M. and Freedman, D. E., A mononuclear transition metal single-molecule magnet in a nuclear spin-free ligand environment, *Inorg. Chem.*, **2014**, *53*, 10716–10721.
84. Liu, J.; Chen, Y.-C.; Liu, J.-L.; Vieru, V.; Ungur, L.; Jia, J.-H.; Chibotaru, L. F.; Lan, Y.; Wernsdorfer, W.; Gao, S.; Chen, X.-M. and Tong, M.-L., A Stable Pentagonal Bipyramidal Dy(III) Single-Ion Magnet with a Record Magnetization Reversal Barrier over 1000 K, *J. Am. Chem. Soc.*, **2016**, *138*, 5441–5450.
85. Guo, F.-S.; Day, B. M.; Chen, Y.-C.; Tong, M.-L.; Mansikkamäki, A. and Layfield, R. A., Magnetic hysteresis up to 80 kelvin in a dysprosium metallocene single-molecule magnet, *Science (80-.).*, **2018**, *362*, 1400–1403.
86. Escalera-Moreno, L.; Baldoví, J. J.; Gaita-Ariño, A. and Coronado, E., Spin states, vibrations and spin relaxation in molecular nanomagnets and spin qubits: a critical perspective, *Chem. Sci.*, **2018**, *9*, 3265–3275.
87. Liu, J.-L.; Chen, Y.-C. and Tong, M.-L., Symmetry strategies for high performance lanthanide-based single-molecule magnets, *Chem. Soc. Rev.*, **2018**, *47*, 2431–2453.
88. Blagg, R. J.; Ungur, L.; Tuna, F.; Speak, J.; Comar, P.; Collison, D.; Wernsdorfer, W.; McInnes, E. J. L.; Chibotaru, L. F. and Winpenny, R. E. P., Magnetic relaxation pathways in lanthanide single-molecule magnets, *Nat. Chem.*, **2013**, *5*, 673–678.
89. Rinehart, J. D. and Long, J. R., Exploiting single-ion anisotropy in the design of f-element single-molecule magnets, *Chem. Sci.*, **2011**, *2*, 2078.
90. Rawson, J. M.; Banister, A. J. and Lavender, I., The Chemistry of Dithiadiazolylium and Dithiadiazolyl Rings. In: *Advances in Heterocyclic Chemistry*, Academic Press, 1995, vol. 62, pp. 137–247.
91. Banister, A. J.; Bricklebank, N.; Lavender, I.; Rawson, J. M.; Gregory, C. I.; Tanner, B. K.; Clegg, W.; Elsegood, M. R. J. and Palacio, F., Spontaneous magnetization in a sulfur-nitrogen radical at 36 K, *Angew. Chemie (International Ed. English)*, **1996**, *35*, 2533–2535.
92. Frisch, M. J.; Pople, J. A. and Binkley, J. S., Self-consistent molecular orbital methods 25. Supplementary functions for Gaussian basis sets, *J. Chem. Phys.*, **1984**, *80*, 3265–3269.
93. Costa, R.; Valero, R.; Mañeru, D. R.; Moreira, I. D. P. R. and Illas, F., Spin adapted versus broken symmetry approaches in the description of magnetic coupling in heterodinuclear complexes, *J. Chem. Theory Comput.*, **2015**, *11*, 1006–1019.
94. Noodleman, L., Valence bond description of antiferromagnetic coupling in transition

metal dimers, *J. Chem. Phys.*, **1981**, *74*, 5737–5743.

95. Schäfer, A.; Huber, C. and Ahlrichs, R., Fully optimized contracted Gaussian basis sets of triple zeta valence quality for atoms Li to Kr, *J. Chem. Phys.*, **1994**, *100*, 5829–5835.
96. Schäfer, A.; Horn, H. and Ahlrichs, R., Fully optimized contracted Gaussian basis sets for atoms Li to Kr, *J. Chem. Phys.*, **1992**, *97*, 2571–2577.
97. Gupta, T.; Rajeshkumar, T. and Rajaraman, G., Magnetic exchange in {GdIII-radical} complexes: Method assessment, mechanism of coupling and magneto-structural correlations, *Phys. Chem. Chem. Phys.*, Royal Society of Chemistry, 2014, pp. 14568–14577.
98. Goodenough, J. B., *Magnetism and the Chemical Bond*, John Wiley & Sons, Ltd, New York, 1963.
99. Vieru, V.; Iwahara, N.; Ungur, L. and Chibotaru, L. F., Giant exchange interaction in mixed lanthanides, *Sci. Reports 2016 61*, **2016**, *6*, 1–8.
100. Gould, C. A.; Mu, E.; Vieru, V.; Darago, L. E.; Chakarawet, K.; Gonzalez, M. I.; Demir, S. and Long, J. R., Substituent Effects on Exchange Coupling and Magnetic Relaxation in 2,2′-Bipyrimidine Radical-Bridged Dilanthanide Complexes, *J. Am. Chem. Soc.*, **2020**, *142*, 21197–21209.